Arabian Journal of Chemistry (2020) 13, 5118–5136

King Saud University

Arabian Journal of Chemistry

www.ksu.edu.sa
www.sciencedirect.com

ORIGINAL ARTICLE

Performance evaluation of the different nano-enhanced polysulfone membranes via membrane distillation for produced water desalination in Sert Basin-Libya

Osamah M.A. Shahlol [a], Heba Isawi [b,*], Mohamed G. El-Malky [c], Abd El-Hameed M. Al-Aassar [b], Adel El zwai [d]

[a] *Faculty of Natural Resources, Al-Jufra University, Libya*
[b] *Desert Research Center, Water Resources and Desert Soils Division, Hydrogeochemistry Dept., Water Desalination Unit, Egyptian Desalination Research Center of Excellence, (EDRC), 1 Mathaf Al Mataria St., P.O.B. 11753, Cairo, Egypt*
[c] *Institute of Environmental Studies and Research Ain-Shams University, Abbassia, Cairo, Egypt*
[d] *Reservoir Engineering Superintendent, AGOCO, Libya*

Received 9 December 2019; accepted 16 February 2020
Available online 4 March 2020

KEYWORDS

Polysulfone modified membrane;
Membrane distillation;
Nanocomposites;
Polyethylene glycol;
Surface modification;
Produced water desalination

Abstract A Polysulfone-Polyethylene glycol (PS/PEG) flat sheet membrane was prepared by phase inversion technique. Dimethyl Formamide (DMF) was utilized as a solvent and deionized water was utilized as the coagulant. Polyethylene glycol (PEG) of a various dose of PEG 2000 was utilized as the polymeric improvers and as a pore-forming agent in the casting mixture. The single-walled carbon nanotube (SWCNTs), multi-walled carbon nanotube (MWCNTs), aluminum oxide (Al_2O_3) and copper oxide (CuO) nanoparticles (NPs) were utilized to improve the PS/PEG membrane performances. The characterizations of the neat PS, PS/PEG, PS/PEG/Al2O3 (M1) PS-PEG/CuO (M2), PS-PEG/SWCNTs (M3) and PS/PEG/MWCNTs (M14) nanocomposite (NC) modified membranes were acquired via Fourier-transform infrared analysis (FTIR), water contact angle estimation (WCA), scanning electron microscope (SEM), dynamic mechanical analyzer (DMA) and thermogravimetric analysis (TGA). Enhanced Direct contact membrane distillation (EDCMD) unit was used for estimating the efficiency of the performance of the synthesized NC membranes via 60 °C feed synthetic water and/or saline oil field produced water samples containing salinities 123,14 mg/L. Adjusting the operational procedures and water characteristics confirmed a high salt rejection of 99.99% by the synthesized NC membranes. The maximum permeate flux

* Corresponding author.
E-mail address: heba_isawi@edrc.org.eg (H. Isawi).
Peer review under responsibility of King Saud University.

Production and hosting by Elsevier

https://doi.org/10.1016/j.arabjc.2020.02.011
1878-5352 © 2020 Published by Elsevier B.V. on behalf of King Saud University.
This is an open access article under the CC BY-NC-ND license (http://creativecommons.org/licenses/by-nc-nd/4.0/).

achieved in the order of SWCNTs (20.91) > Al_2O_3 (19.92) > CuO (18.92) > MWCNT (18.20) (L/m^2.h) with adjusted concentration of 0.5, 0.75, 0.75, 0.1 wt% compared with PS weight, i.e. 16%. The optimum operational circumstances comprised feed and permeate temperatures 60 °C and 20 °C, respectively. The achieved flux was 5.97 L/m^2.h, using brine oil field produced water, via PS/PEG/SWCNTs membrane with 0.5 wt% of SWCNTs. Moreover, the membrane indicated sustaining performance stability in the 480 min continuous desalination testing, showing that the synthesized PS/PEG/SWCNTs NC modified membrane may be of magnificent potential to be activated in EDCMD procedure for water desalination.

© 2020 Published by Elsevier B.V. on behalf of King Saud University. This is an open access article under the CC BY-NC-ND license (http://creativecommons.org/licenses/by-nc-nd/4.0/).

1. Introduction

Global request for freshwater is predicted to increase in the future owing to speedy population expansion (Elimelech and Phillip 2011). The membrane separation has been reflected to be the most significant contraptions for water desalination worldwide. Its procedure offers easy operation, great stability, low-cost energy and high efficiency (Isawi 2018). Freshwater shortage has continued a developing issue owing to increasing potable water demand of global population and continuing industrial improvements. Great efforts have been assumed to increase the freshwater resources whichever via discovering new water resources or via reprocessing of wastewater via different water treatment technologies (Pana et al., 2019). Confirming safe and clean water resource is an essential right for the sustainability of mankind. Regrettably, climate changes, population growing, environmental effluence, industrial enlargements, to name a scarce are creating freshwater shortage an exceptional crisis of the 21stcentury (Isawi et al., 2016a & Homaeigohar and Elbahri 2017). In crude oil producing operations, it is often necessary to manage saline water that is produced with the crude oil. This saline water must be detached from the crude oil and to get rid of in a technique that does not disturb ecological criteria. In offshore regions, the governing regulatory body specifies maximum dissolved solids content in water that is permitted to be discharged overboard (Ahmadun et al., 2009). Desalination of oil field produced water can potentially be responsible for a new source of water and will eliminate the threats of oil field discharges on environs (Zhang et al., 2017).

Membrane distillation (MD) is a process that utilized variances in vapor pressure to permeate water vapor via the hydrophobic porous membrane and rejects non-volatile constituent existing in the water (Wu et al., 2018). MD is popular for water desalination owing to several advantages: (a) lesser functioning hydrostatic pressures, (b) lower operative temperatures than that of conventional distillation procedure (c) high rejection issues i.e. 100% (hypothetical) when solutions involving nonvolatile solutes, (d) fewer imperative membrane's mechanical possessions, and (e) membrane fouling in MD is a less continual problem when compared to the pressure driven procedures as reverse osmosis (RO). Enhanced direct contact (EDC) MD is the unpretentious MD conformation and is extensively working in the water desalination. In EDCMD, the hot feed solution is in direct contact with the hot membrane side surface consequently, evaporation occurs at the feed membrane surface. The vapor is moved via the pressure alteration through the membrane to the permeate side and condenses into the membrane unit.

The polymeric constituents are the foremost components in membrane preparation. The commonly considered polymeric membranes as polyvinylidene fluoride (PVDF), polyethersulfone (PES), polypropylene (PP), and polysulfone (PS) are considered to be favorable to water treatment and water desalination techniques. PS is of semi-hydrophobic in nature and is generally utilized in the applications of biology, medicine and pharmacy because of its high stability on a diversity of techniques. The advantages of PS are highly stability, rigidity; drag out resistance, and displays good thermal stability. PS is used as membrane material owing to its stability for high chemical resistance and allowance wide range of pH and it is capable of acting as a good oxidizing constituent on the diversity of pH range and also allows the process to function at temperature up to 80 °C. Conversely owing to its hydrophobic nature, PS membrane is extremely disposed to fouling problem (Ma et al., 2011). PS is a prevalent membrane material because of its mechanical strength, thermal stability, and chemical deactivation. The PS membranes are favorable as a result of their maximum handling capacity, high efficiency, and low energy necessity, low cost for large-scale manufacture, high thermal and/or chemical confrontation, and brilliant physical/-chemical stabilities (Ang et al., 2015).

Properties and structure of membranes created via phase inversion technique be influenced by many features. Additives are one of the highest features and play crucial role in the formation of membrane structure via increasing or inhibiting of macrovoid creation, improving pore creation, enhancing pore interconnectivity, and/or presenting hydrophilicity (Mosqueda-Jimenez et al., 2004 & Jung et al., 2004).

Modification of membrane through enhancement of membrane structure, mechanical possessions and performance has been significantly considered to improve the membrane separation technique (Abdelrasoul et al., 2015 & Zeng et al., 2018). Consistent with previous studies, the use of additive is one of the enhancement approaches which are commonly utilized to modify membrane structure for instance to improve pore structure, enhancing pore interconnectivity, surface roughness, improving hydrophobicity and hydrophilicity of the membrane (Liu et al., 2011 & Lau et al., 2012). Moreover the strong influence of additives could simply interrupt and change the membrane structure creation through phase inversion procedure via influencing the entry and discharge of the solvent and coagulant. The modifications of membrane structure intensely affect the membrane possessions and performance

and the improver addition is the simplest and greatest economical technique to inhibit fouling of greatest hydrophobic membrane.

The commonly utilized additives are macromolecular as polyvinylpyrrolidone (PVP), polyethylene oxide (PEO), polyethylene glycols (PEG), organic compounds such as alcohols, glycerol, dialcohols, inorganic salts such as $ZnCl_2$, water and LiCl. The additive can be a single constituent or a mixture. PEG as additive is less commonly operated compared to PVP, nonetheless it could show a comparable role in the creation procedure, performing as a macrovoid suppressor and charitable the membrane a hydrophilic properties and used to enhance membrane selectivity (Xu et al., 1999). A main role of the PEG could be a pore former and macrovoid oppressor. Saljoughi et al. 2010 found that small molecular weight PEG improver in the cast solution sheet can enhance porosity, permeability, as well as consecutively chemical and thermal stability of the synthesized cellulose acetate membranes. Membrane with PEG of greater molecular weight has greater pure water flux and greater hydraulic permeability owing to more porosity.

Recently, a substantial deliberation has been paid to the formation of nanocomposite membrane for water desalination and treatment as a result of its improved outputs containing high water performances. Recently, nanoparticles have concerned considerable attention as progressive strengthening fillers to improve membrane possessions (de Lannoy et al., 2013). A recent procedure uses metal oxide nanoparticles to enhance the membrane antifouling and performances. Between these nanoparticles are titanium dioxide (TiO_2) (El-Aassar et al., 2019), Znic oxide nanoparticles (ZnO NPs) (Isawi et al., 2016b), grapheme oxide (GO) (Lai et al., 2016), nanoclay (Isawi 2019), Fe_3O_4 nanoparticles, and silver nanoparticles (Daraei et al., 2012 & Zeng, et al., 2018) aluminum oxides (Al_2O_3) (Isawi 2019), silica dioxide (SiO_2) (El-Aassar et al., 2019 & Huang et al., 2017a & Huang et al., 2017b), CuO nanoparticles (Isawi 2019) and carbon nanotube (CNTs) (Huang et al., 2020 & Zeng et al., 2016 & Zeng et al., 2015). The novel carbon ingredients such as CNTs have concerned worldwide technological attention and scientific (Salehi et al., 2012). The multi-walled and single carbon nanotube (MWCNTs and SWCNTs) have unique possessions such as high surface area, excellent mechanical possessions and good hydrophilicity, CNTs has become the ideal constituent for strengthening mechanical possessions and enhancing the permeability of composite membranes. Furthermore, above the past various years, highly hydrophilic Al_2O_3, CuO NPs, SWCNTs and MWCNTs are extensively utilized in the creation of the nanocomposite membrane. Testing this assumption is crucial to compare the NC modified membrane performances, mechanical possessions, antifouling possessions, and for the oil field produce water desalination using various nanocomposite membranes at identical circumstance. Conversely, there are several problems in synthesized mixed matrix membranes via metal oxides and CNTs, as low diffusion of CNTs in organic solvents, various polymers and low interface interaction among the polymer matrix and the nanofiller (Celik et al., 2011). Consequently, the chemical structure membrane modification via an additive is a favorite implementation to develop the distribution ability of metal oxides and CNTs to produce a homogeneous NC membrane. Simultaneously, PEG, metal oxides and CNTs can be simply attached and modified various hydrophilic functional groups via utilizing membrane modification for uniform dispersal of NPs in the polymer medium. The MWCNTs, SWCNTs, Al_2O_3, and CuO NPs possess an OH group on their surface, which links with the functional groups in the PS/PEG polymer matrix via a hydrogen or covalent bond (Zheng et al., 2005 & Isawi et al., 2016b) facilitating this incorporation, and increasing the stability of the NPs on the membrane surface.

This work studied the effects of PEG (2000 MW) was used as a polymeric additive in 16% PS and 84% DMF to develop the morphological structures, surface properties and performances of polysulfone membrane resulting PS/PEG membrane. Additional preparation and modification of PS/PEG flat sheet membranes using different nanomaterials such as multiwall carbon nanotube (MWCNTs), single wall carbon nanotube (SWCNTs), Al_2O_3, and CuO were achieved. The synthesized membranes were characterized via FTIR spectroscope, DMA, contact angle measurement, TGA and SEM. The performance of the synthesized NC modified membranes in water desalination was estimated via studying the impact of membrane preparation circumstances, feed water features and operating circumstances. Furthermore, the stability of the synthesized PS/PEG/SWCNTs NC modified membrane compared to Neat PS membrane will be examined using EDCMDS for water desalination. The optimum operational circumstances will be applied using brine oil field produced water sample using PS/PEG/SWCNTs NC modified membrane to show the novelty of the selected membrane for desalination of such hyper saline water sample. The EDCMDS tests were succeeded utilizing a novel pilot-scale MD unit. The feed water was synthetic NaCl solution with various salinities. Subsequently, the applicability of the prepared PS/PEG/SWCNTs NC modified membrane was showed using natural oil field produced water sample with salinity 123,136 mg/L collected from Sarir oil field in Sirt basin, Libya.

2. Experimental

2.1. Materials

The membrane substrate was prepared from Polysulfone PS (Udel P 3500 LCD MP7, MW = 77000, Density = 1.24 g/ml at 25 °C) using N,N-dimethylformamide (DMF, 99.8%, Density = 0.94 g/ml at 20 °C) as a solvent using the phase inversion method. Polyethylene glycol (PEG, MW = 2000) used as pore former agent. All chemicals were gotten from Sigma–Aldrich. The MWCNTs and SWCNTs with length of 0.1–10 μm, inner length of 2–6 nm and outer length of 10–15 nm as well as aluminum oxide (Al_2O_3) NPs and copper oxide (CuO) NPs Al_2O_3 and CuO were delivered by Sigma-Aldrich. Sodium chloride was used as a representative solute for salt rejection measurements. The pure water was supplied from an ultra-pure water system (PURELAB Option-K system, UK), with a resistivity of greater than 15 mΩ-cm.

2.2. Preparation of neat and nanomaterials modified hydrophobic polysulfone membrane

The schematic graph of the membrane fabrication procedure is presented in Fig. 1. The micro-porous PS membrane was synthesized via the phase inversion technique. The PS membranes

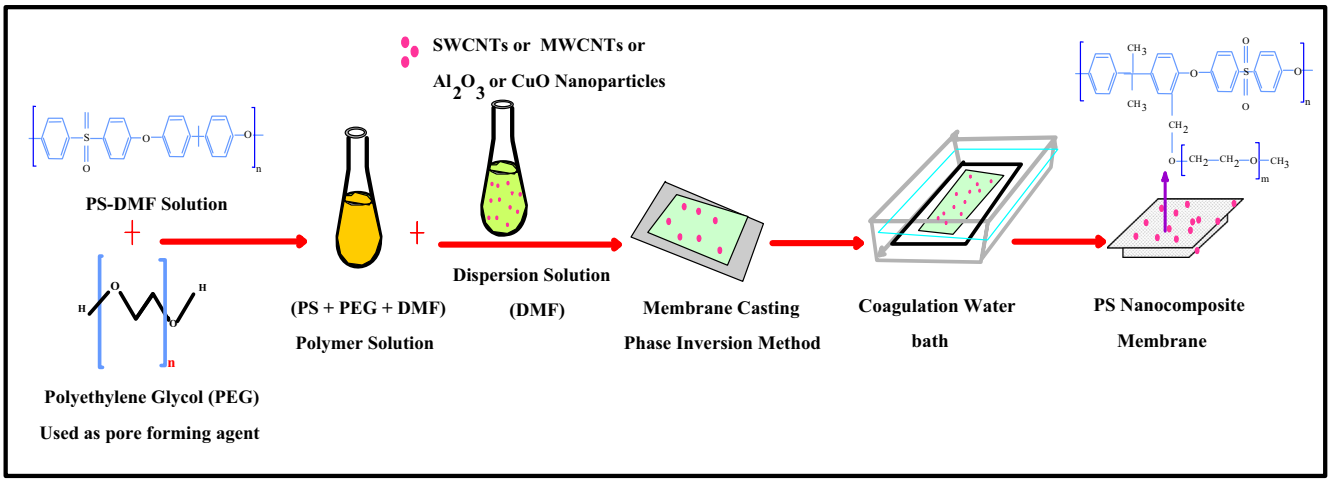

Fig. 1 Schematic representation of PS nanocomposite membranes.

were cast from a homogeneous polymer solutions having different PS pellets concentration (12–18 wt%, w/v) and 88–82 wt% DMF as a solvent, the casting solution was gently heated 3–4 h at 80–90 °C in a clear glass bottle with constant stirring until the homogenous solution was obtained then saved overnight for degassing at 25 °C Fig. 1. To improve the PS membrane performances, the PEG with different amounts (0.5–3.5 as a wt% of PS concentration) were added to PS mixture. A variety of freshly unequal NC PS membranes were prepared using diverse nanoparticles such as MWCNTs, SWCNTs, Al_2O_3, and CuO NPs. DMF was utilized as a solvent to assist in the nanoparticles dispersion via sonication for (30 min) procedure in order to have good distribution of nanoparticles in polymer matrix. To synthesize the PS/PEG/MWCNTs, PS/PEG/SWCNTs, PS/PEG/Al_2O_3 and PS/PEG/CuO NC modified membranes, an applicable amount of MWCNTs (0.0125–0.1 wt%), SWCNTs, Al_2O_3 and CuO NPs (0.25–1 as a wt% of PS concentration) were mixed with 15 mL of DMF solutions, subsequent the mixtures were sonicated into an ultrasonic bath at 25–30 °C for at least 30 min to assist the dispersal of the MWCNTs, SWCNTs, Al_2O_3, and CuO NPs into the solvent matrix then added to PS/PEG mixture. Then these mixtures heated and stirred for 3–4 h to get best homogenous nano-polymer matrix then kept overnight for degassing. The resultant polymer solution was casted on a glass plate with different thicknesses 50–200 μm using TQA Automatic film applicator, the membrane was allowed to dry and the solvent was regularly vaporized in air for 30 s, relative humidity (10–60%), and directly immersed into a deionized water bath (25 °C), as shown in Fig. 1. After precipitation (2–3 min) the synthesized membranes were washed using deionized water, dried completely and kept in dry place until performance and characterization processes. The resulting neat PS, PS/PEG, PS/PEG/Al_2O_3 (M1), PS/PEG/CuO (M2), PS/PEG/SWCNTs (M3) and PS/PEG/MWCNTs (M4) NC modified membranes revealed in Table 1.

The schematic diagram in Fig. 1 shows that the incorporation of the different nanomaterials such as MWCNTs, SWCNTs, Al_2O_3, and CuO NPs, with PS/PEG polymer matrix could have been recognized via one of two procedures. Firstly, the influence of moisture and humidity may have led to the creation of OH groups on the surfaces of the NPs, so that, a covalent bond formed through the chemical reaction of the functional group of PS/PEG and the different nanomaterials OH group (Zheng et al., 2005). The second possible procedure is the creation of an hydrogen-bond among the surface OH groups of the different nanomaterials, and the oxygen in the PS/PEG functional groups (Isawi et al., 2016b).

Table 1 The types of membranes.

Membrane Types	Membrane notation	Nanomaterials (wt%)
Neat PS	Pure PS	PS Conc. 16%
PS/PEG	PS/PEG	PEG Conc. 2%
PS/PEG/Al_2O_3	M1	Al_2O_3 0.75%
PS/PEG/CuO	M2	CuO 0.75%
PS/PEG/SWCNTs	M3	SWCNTs 0.5%
PS/PEG/ MWCNTs	M4	MWCNTs 0.1%

2.3. Characterization of the membranes

The membranes were characterized via FTIR, the contact angle, mechanical properties, SEM and TGA. FTIR analysis of the synthesized membranes was achieved via a Bruker Vertex70 FT-IR spectrophotometer model. The contact angle (CA) was utilized to control the membrane surface hydrophilicity and hydrophobicity at 25 °C via the sessile drip technique on a Drop Form Analyzer-DSA25, Germany contact angle aperture. A water drop was located onto the membrane surface after air-dried by deionized water with a digital micro-syringe, at least 3–5 measurements at diverse locations were attained for every membrane and the average rate was considered and listed. The mechanical possessions of the membrane samples were determined with Universal Testing Apparatuses (Module DMA Q800 V21.1 Build 51-Controlled Force, DMA), where the dynamic stress and strain were deliberated at 25 °C. The tensile examinations were utilized to evaluate the Young's modulus and strain at breakage of samples at the rate of 10 mm/min. The prepared membrane sections were cut into small rectangles with a measurement of (20 × 13 × 0.15 mm), and located vertical to one another in

between two automatic fascinating units of the sample, leaving a 3 cm sample extent for mechanical loading. The width of the membrane sections was considered with an automatic micrometer with a precision of 1 μm. Young's modulus (Mega Pascal, M pa) was considered via the following equation:

$$\text{Young's modolus (Mpa)} = \text{Stress/Strain} \quad (1)$$

The scanning electron microscope (SEM, Quanta FEG) was used to imagine the membrane's surface features. To observe membrane cross-sections, membrane samples were ready by cracking in liquid nitrogen. The TGA of prepared membranes was carried out by using a Shimadzu TGA system of type TGA-50H using N_2 with flow rate 20 mL/min and temperature rate holder 10 °C/min sample weight varied in rang (1–2 mg).

2.4. Sample collection and analysis

The produce water sample was gathered from water basin in the area under investigation. The produce water sample was gathered in a clean polyethylene bottle and exposed to the measurements of chemical and physical possessions of water samples. The chemical investigates of produce water sample were achieved via the main laboratory of the Desert Research Center (DRC) in Cairo, Egypt. The gathered and analyses samples joint to the standard approaches of the ASTM, 2002; Hem, 1991; APHA, 1998; Brown et al., 1970. The physical possessions of produce water samples were perceived via assessing the specific electrical conductance (EC) via EC meter (LF 538, WTW, USA Model) and expressed in micro-mhos for every centimeter (μS/cm) at 25 °C, and pH value was determined using Jenway, UK 3320 pH meter.

The chemical possessions were estimated through calculating total dissolved salts (TDS), Ca^{2+}, Mg^{2+}, Na^{+}, K^{+}, CO_3^{2-}, HCO_3^{-}, SO_4^{2-} and Cl^{-} ions concentration. The achieved chemical data are expressed in milligram per liter (mg/l) or part per million (ppm). Analytical accuracy for the measurements of cations and anions, gotten from ionic balance error (IBE), was calculated in terms of ions expressed in milli-equivalent per liter. The significance of IBE is detected to be contained by a limit of ±5% (Domenico and Schwartz 1990). Total dissolved solids (TDSs) were calculated via multiplying the EC (ds m^{-1}) via a factor of 640 (Subramani et al. 2005).

2.5. The EDCMD experimental setup and membrane performance assessment for desalination techniques

The enhanced direct contact membrane distillation system (EDCMDS) experimental outfit is schematically described in Fig. 2. The module designed for membrane performance comprised of two sections, the feed tank and the permeate tank where (P_f, P_p, T_f and T_p) represent feed and permeate pressure and temperature respectively. The sections were prepared from polyacrylic to repel the corrosion via feed solutions. The module stood horizontally to facilitate the feed solution flowed through the bottom section of the module while the cooling water distributed through the upper section. The feed and permeate separated via a membrane with effective area of 0.006 m^2 Fig. 2. The thermostatic hot feed water bath was intended for monitoring the hot current. Conversely, the cooler (Chiller NESLAB CFT-75 Cooled Re-circulator model, USA) was intended for detecting the cold current. The EDCMDS consist of two flow meters (Blue-White F-550 model, USA) and (Green-life Drinking Water model, USA) were applied with ranges of 1 to 7 L/min and 5 to 35 L/min for permeate water feed currency, respectively.

The model composed of two centrifugal pumps and two pressure gauges (WSGSOLO model 100 mm radial) with pressure varied from −30 to 70 psi were applied. Furthermore, four thermocouples with an accuracy ±0.1 °C were utilized

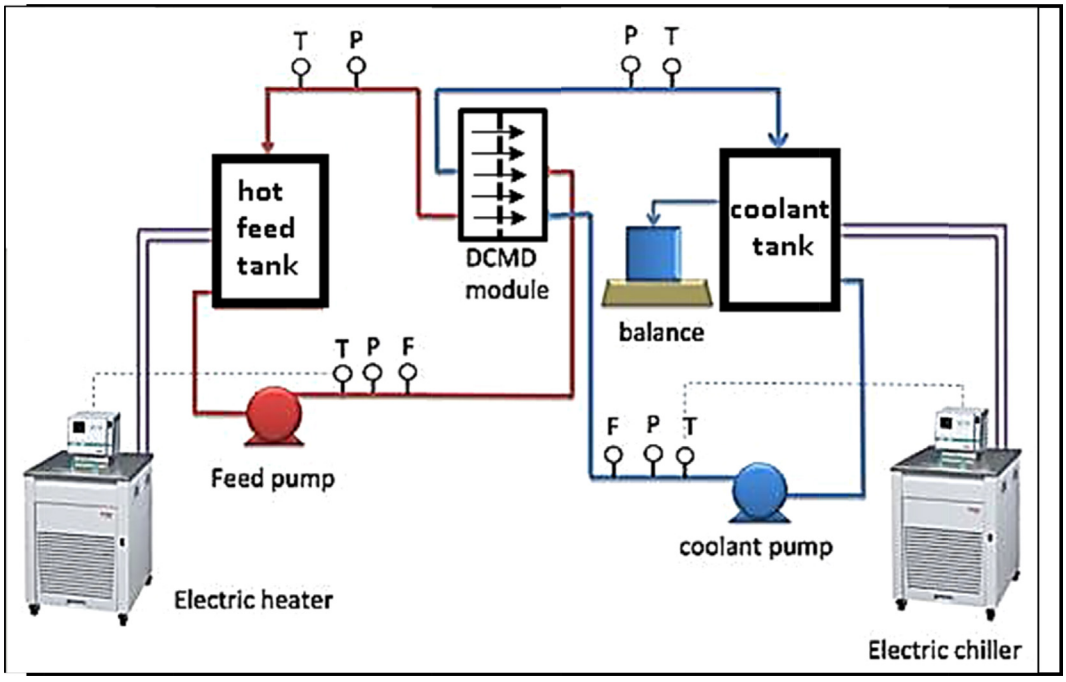

Fig. 2 Diagram of DCMD experimental unit used in this study.

for estimating the temperatures of both currents. The vessels of 4.8 and 15L were utilized for cold and hot currents, respectively. The feed and permeate solutions were comprised in double-walled tanks and distributed via the membrane module using centrifugal pumps. All gained data from the synthesized membranes with stable flux were informed as mean value of the calculated flux every one hour over a 3–5 h period. The amount of pure water taken was estimated via water conductivity utilizing an electrical conductivity meter (EC470-L, ISTEK, Korea) which reported as an increasing in permeate conductivity specified that liquid water passes via the membrane so that outcome is rejected, in other words that is the salt rejection of all membranes was 99.99%. To examine the existence of leakages in the EDCMDs model, in addition to the membrane hydrophobicity, the volume in the graduated cylinder was detected when only the hot stream was recounted for as a minimum 30 min before beginning the experiment. Through the experiments, the feed was at 0.5 bars and its flow rate was various between 0.5 and 1 L/min, while the feed temperature was ranged between 40 and 60 °C and the permeate temperature was in the variety of 20 to 10 °C and the feed water salinity is 20,000 mg/L. The membranes capability to achieve water desalination was adjudged in terms of water flux (J_w, L/m^2.h) and salt rejection (S_R%), using a laboratory enhanced direct contact membrane distillation system (EDCMDS). Pure water flux was measured, followed by EDCMDS test with a synthetic NaCl feed solutions were used with diverse salinities ranged from 20,000 to 200,000 mg/L. The disintegrate salt in the feed and permeate water were determined via a conductivity meter. The measurements of water flux and salt rejection were occupied 30 min after purification to confirm a steady state had been touched. Furthermore, a brine oil field produced water sample, with a total dissolved solid concentration of 123,136 mg/L collected from Sarir oil field in Sirt basin, Libya, was accustomed study and compare the membranes. The salt retention and permeate water flux were considered from the next equations:

$$R = \left(1 - \frac{Cp}{Cf}\right) \times 100 \quad (2)$$

$$Jw = \frac{Vp}{At} \quad (3)$$

where R the salt retention, and C_p and C_f the concentrations of permeate and feed solution, respectively, J_w is the water flux (L/m^{2}h), V_p the permeate volume (L), A the surface membrane area (m^2), t the separation time (h).

3. Results and discussion

3.1. Characterization of membranes

3.1.1. FTIR analysis

FTIR spectroscopy can be responsible for an appropriate and operative technique to determine the functional groups of the neat and modified PS membranes. FTIR was achieved to approve the effective preparation of PS membranes, to verify the successful incorporation of PEG with PS support membrane where the PEG not only doing as a pore former but also modify the conformation of PS molecules, affect the dispersive status of polymer and the dynamic rate of membrane formation progress. FTIR was succeeded to determine the functional groups in the PS/PEG NCs modified membranes via doping different nano-materials such as Al_2O_3, CuO, SWCNTs, MWCNTs. The FTIR spectra of the neat PS, PS/PEG, M1, M2, M3, and M4 are shown in Fig. 3.

It is observable that all synthesized membranes contained very comparable functional groups because of the presence of identical peaks. This is because of the chemical constructions of the synthesized membranes. The absorption bands of the material relates to the PS functional groups, being in good matches with standard PS at 1014 cm^{-1} related to SO_3H group, 1105 cm^{-1} corresponding to C-O. The FTIR displays two bands around~1324 cm^{-1} which can be ascribed to a symmetric stretching vibration of RO = S = OR, corresponding to pure PS (Balta et al., 2012) and the band at 1240 cm^{-1} is illustrative of an asymmetric stretching vibration of the C − O − C in the aryl ether group (Isawi et al., 2016b). The band at 1488 cm^{-1} is demonstrative of aromatic bond. The bands appear around 2968 and 2879 cm^{-1} due to aliphatic CH and aromatic CH, respectively (Nechifor et al., 2013). The band at 854 cm^{-1} is produced by the hydrogen deformation of *para*-substituted aryl groups (Sadtler, 1980).

All membranes revealed typical bands of PS, i.e., aliphatic C-H rocking peak at 716 cm^{-1} and characteristic peaks at 855, 1015, 1105 and 1170 cm^{-1} were attributed to aromatic hydrogen bending. The specific peak appears around 1410, 1504, and 1585 cm^{-1} which related to C = C aromatic ring stretching and the band appears around 2880 and 2968 cm^{-1} attributed to C-H aliphatic stretching, respectively (Singh et al., 2006). The IR spectrum of PS/PEG, it displayed both the absorption band at 1250 cm^{-1} for C − O − C ether bond of PEG moiety and the aryl-ether bond of PSF moiety (Du

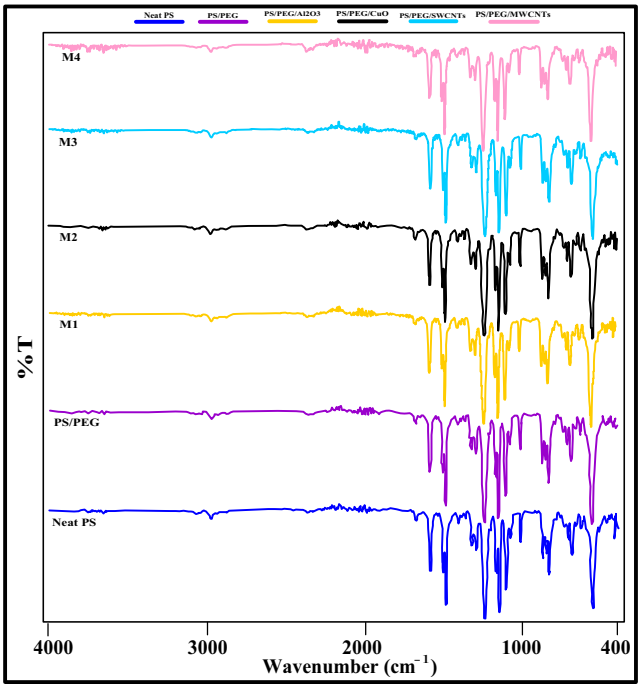

Fig. 3 The FTIR spectra of Neat PS, PS/PEG, PS/PEG/Al_2O_3 (M1), PS/PEG/CuO (M2), PS/PEG/SWCNTs (M3) and PS/PEG/MWCNTs (M4) NC modified membranes.

et al., 2013 & Yuenyao et al., 2016), these are due to the formation of the covalent bond between the PSF moiety and PEG moiety.

By contrast, no additional peaks were observed for the membranes prepared with the adding of PEG. The object for this outcome would be overlapping peaks for PS ether group and C-H stretching (Susanto and Ulbricht 2009).

The incorporated nanoparticles have various oxy-functional groups which might be overlap with neat PS membranes. Absence of their exclusive bands in this study could also attribute to using slight nanoparticles concentration used which might be compacted under PS polymeric chains (Vetrivel et al., 2015).

3.1.2. Contact angle

The contact angle (θ; CA) is the most mutual factor utilized to describe the hydrophilicity and hydrophobicity of membrane surfaces. Hydrophilic membranes have a CA of $0° < \theta < 90°$ while hydrophobic membranes have a CA of $90° < \theta < 180°$. Delineation of contact angle is very essential for membrane distillation. The contact angles of the Neat PS, PS/PEG, PS/PEG/Al_2O_3 (M1), PS/PEG/CuO (M2), PS/PEG/SWCNTs (M3) and PS/PEG/MWCNTs (M4) NC modified membranes are revealed in Fig. 4. Hydrophilicity and permeability of the membrane are two important parameters in membrane separation and permeation procedure and have a contiguous relationship with water reflux and the morphology of membranes. Generally, membrane hydrophilicity is higher while its contact angle is smaller. In Fig. 4, the mean water contact angles for the Neat PS, PS/PEG, PS/PEG/Al_2O_3 (M1), PS/PEG/CuO (M2), PS/PEG/SWCNTs (M3) and PS/PEG/MWCNTs (M4) NC modified membranes were 68 ± 3°, 58 ± 2.5°, 50 ± 3°, 66 ± 1.9°, 70 ± 3° and 73 ± 2.5°, respectively, indicating they possess hydrophilic surfaces. It can be recognized that, the addition of PEG, reduced the contact angle and porosity increases of PS membrane. This is mainly ascribed to the entrapment of PEG in the membrane which leads to the decline of WCA. The higher the hydrophilicity of PS/PEG membrane surface may be because of the higher of oxygen content groups on PS/PEG membrane surface which responsible for the achievement of progressive membrane hydrophilicity. There is a strengthening of the contact angle value for PS/PEG upon doping with primeval hydrophobic MWCNTs and SWCNTs (Okiel et al., 2016). In contrast, the incorporation of CuO and Al_2O_3 reduced the contact angle of PS/PEG NC membrane due to oxide forms of these nanoparticles that might do as active materials on the PS/PEG NC membrane surface and form hydrogen bonds with H_2O (Madaeni et al., 2013). The contact angles were arranged as in order: (M4) > (M3) > neat PS > (M2) > PS/PEG > (M1).

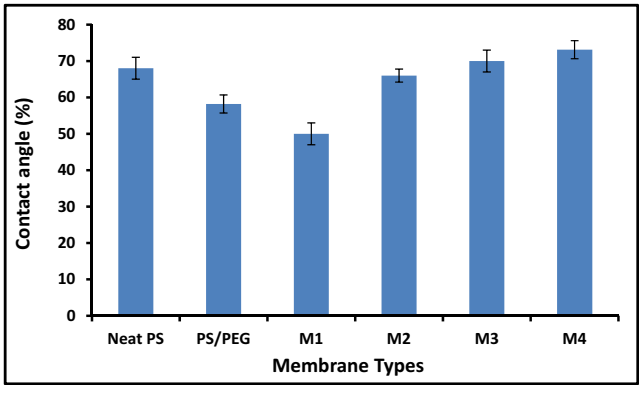

Fig. 4 The contact angle of Neat PS, PS/PEG, PS/PEG/Al_2O_3 (M1), PS/PEG/CuO (M2), PS/PEG/SWCNTs (M3) and PS/PEG/MWCNTs (M4) NC modified membranes. All the experiments were done at room temperature (25 °C).

This is mostly owing to the hydrophilic nature of the Al_2O_3 and CuO nanoparticles that also contributed to producing membrane surface more hydrophilic. The lower the water contact angle of M2 and M1 mainly attributable to the interaction between the PS/PEG polymer matrix and strong base, which can initiate various hydrophilic oxy-functional polar groups, such as hydroxide radical ($HO^{\bullet}$) and carboxyl (COOH) groups and incorporation of PEG owing to retains a less negative charge on the membrane superficial that improves the hydrophilicity of the PS membrane (Isawi, 2019). This consideration mainly attributable to the existence of active hydrophilic functional groups on the PS/PEG membrane surfaces, which also helps to enhance the antifouling belongings. The incorporation of MWCNTs and SWCNTs into membrane matrix enhanced the smoothness and increased the hydrophobicity of the PS/PEG membrane surfaces which leads to improve the water flux of the PS/PEG in membrane distillation system. The hydrophobicity of the membrane owns will mainly conclude its suitability for a DCMD application. Extremely hydrophobic membranes, specified via a measured high contact angle, will repel wetting and oppose liquefied H_2O from incoming the membrane pores. Conversely, hydraulic pressure of the bulk H_2O on both side of the membrane can overcome the inherent surface rigidity and permit feed water to pass via the PS/PEG NCs membrane. As the membrane does not compromise slightly resistance to salt passage, slightly feed water ingoing the pores will cause saline permeate and be seen as reduced salt rejection. Consequently, the higher the hydrophobicity of the PS/PEG NCs membranes, the greater the pressures inside a membrane unit that can be resist before salt rejection is influenced. These outcomes show the recently obtainable PS/PEG/SWCNTs (M3) and PS/PEG/MWCNTs (M4) NC modified membranes are able to conserve high water flux and salt rejections at the higher pressures accompanying with required flow rate (Dow et al., 2008).

The contact angle of the M4 NC modified membrane shows a higher value which meant the other NC modified membranes had poor hydrophobicity compared to the M4 membrane. Alternatively, the slight amount of large pores occurred on the membrane surface could also convince membrane fractional wetting and reduce the PWF.

3.1.3. Mechanical properties analysis

The mechanical properties include tensile strength (Mpa), elongation at break (%) and young modulus (Mpa) of the neat PS, PS/PEG, PS/PEG/Al_2O_3 (M1), PS/PEG/CuO (M2), PS/PEG/SWCNTs (M3) and PS/PEG/MWCNTs (M4) NC modified membranes are revealed in Fig. 5 and Table 2. According to Fig. 5 and Table 2, it is observable that there is a decline in tensile strength for all NCs modified PS/PEG membranes relating to the neat PS membrane. The Young modulus

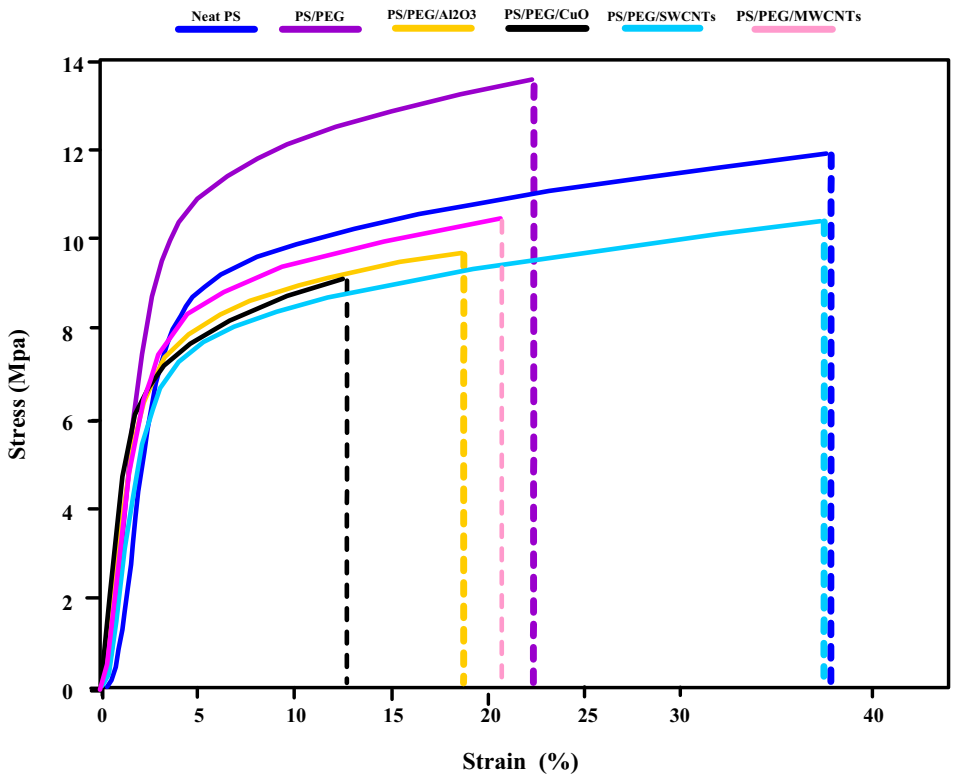

Fig. 5 The Stress-Strain curve of Neat PS, PS/PEG, PS/PEG/Al_2O_3 (M1), PS/PEG/CuO (M2), PS/PEG/SWCNTs (M3) and PS/PEG/MWCNTs (M4) NC modified membranes.

Table 2 The mechanical Properties and the calculated Young's modulus (MPa) of Neat PS, PS/PEG, PS/PEG/Al_2O_3 (M1), PS/PEG/CuO (M2), PS/PEG/SWCNTs (M3) and PS/PEG/MWCNTs (M4) NC modified membranes.

Membrane type	Young's modulus (MPa)	Maximum elongation (%)	Tensile strength (MPa)
Neat PS	354.2	37.6	12
PSF/PEG	434.6	22.3	13.6
M1	387.8	18.6	9.7
M2	455.3	12.5	9.1
M3	313.9	37.2	10.4
M4	315	21.04	10.54

declined for modified membranes with the various nanoparticles except M2. This reduction is owing to the nanoparticles nature and its concentration (Mo et al., 2007).

The membranes own tensile strength values in the following order: PS/PEG > neat PS > M4 > M3 > M1 > M2, while the order for elongation break was neat PS > M3 > PS/PEG > M4 > M1 > M2 and Young's modulus was M2 > PS/PEG > M1 > neat PS > M4 > M3 NCs modified membranes. It is significant to refer that there is a slightly enhanced in tensile strength, elongation break and Young modulus for all NC modified membranes, this mainly ascribed to cross-linking possessions in the alkyl group, and the stiff aromatic structure in the membrane backbone to tolerate the stress of the membrane capacity. The mechanical properties of the NC modified PS/PEG membranes has been improved via the addition of a diminutive amount (0.1–0.75 wt%) of NPs inside the membrane surface, producing improved flexibility and strength. The mechanical possessions of the NC modified PS/PEG membranes depend mainly on the membrane micro-structure and intermolecular forces operative (Augustine et al., 2014). Furthermore, the addition of small amount of MWCNTs and SWCNTs to the PS/PEG membranes create them more crystalline, and the crystalline membrane is stronger than the amorphous ones and leads to a uniform dispersion of MWCNTs and SWCNTs in the membrane matrix which offers greater uniform stress spreading, reduced creation of stress-concentration centers, and subsequently improve the mechanical possessions of the NC membranes (Moniruzzaman et al., 2007). Additionally, the linkage bond among the nanoparticles and PS/PEG membrane generates flexible spacers on the nanoparticle-membrane interface, which improves the rigidity of the NC membrane chain.

3.1.4. Thermo-gravimetric analysis

Thermo-gravimetric analysis (TGA) was achieved for Neat PS, PS/PEG, PS/PEG/Al_2O_3 (M1), PS/PEG/CuO (M2), PS/PEG/SWCNTs (M3) and PS/PEG/MWCNTs (M4) NC modified membranes, as displayed in Fig. 6.

It is clear that all the membranes revealed a slow reduction in the range from 100 °C to 500 °C earlier the vertical decline. When the temperature touches 500–600 °C, weight loss (%) occurs quickly as a result of the degradation of PS into H_2O and CO_2 (Leo et al., 2012). This attitude was participated via both the removal of moisture restricted into the membranes and the thermal constancy of polymeric substantial (Khalkhali and Keivani, 2005). It is noticeable that the

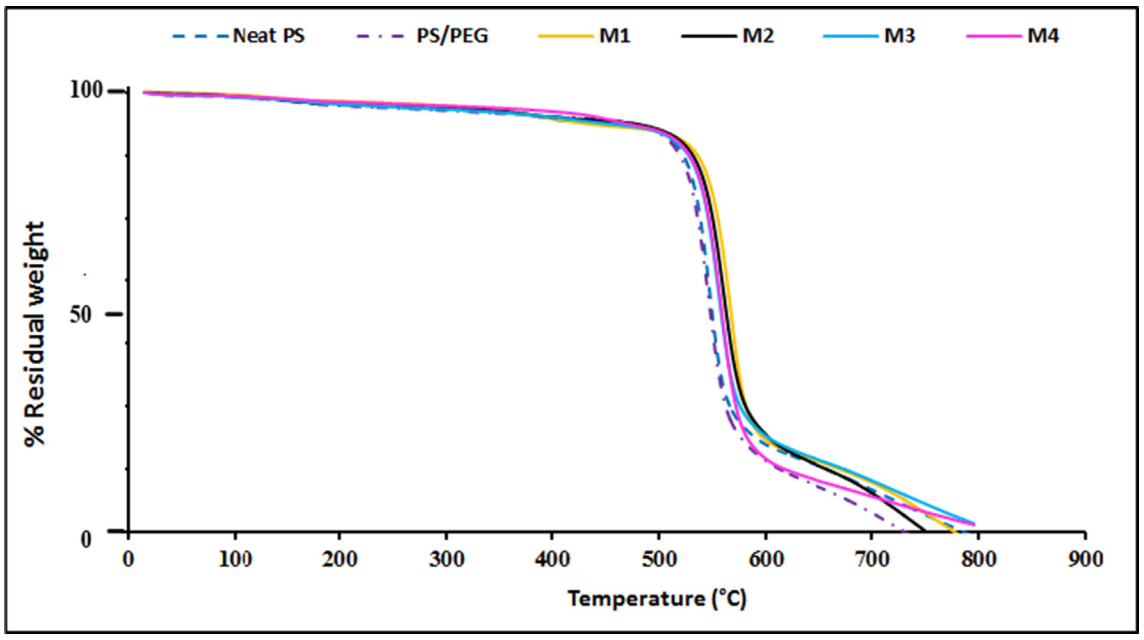

Fig. 6 TGA curve of the Neat PS, PS/PEG, PS/PEG/Al_2O_3 (M1), PS/PEG/CuO (M2), PS/PEG/SWCNTs (M3) and PS/PEG/MWCNTs (M4) NC modified membranes with the heating rate of 10 °C/min.

decomposition of all synthesized membranes happened via two phases of weight loss. The first phase started in temperature ranged from 500 °C to 600 °C, this mainly attributed to the lower molecular weight composites (carbon dioxide, carbon monoxide), binding H_2O, initiator residuals fragments (Tang et al., 2006) and the splitting of $-SO_3H$ groups as well as the evaporation of additives as DMF. The second phase started from 600 to 790 °C which mainly owing to the incision of the polymer main chain. It is remarkable that the S = O group in the central chain of the PS appears to procedure an intermolecular H-bond with H_2O. A weight loss in all membranes above 700 °C is concerning to the splitting of the C-atoms at higher than 650 °C. The thermal constancy of the PS modified membranes are owing to its ideal chemical structure, which is consist of aromatic benzene rings, mostly identified to be extremely resistant to increases in temperature (Isawi et al., 2016b). The TGA curve of NCs modified PS/PEG membrane presented in Fig. 6 mention that thermal decomposition was shifted to a higher temperature than neat PS. The TGA curves display that the incorporation of different NPs significantly improves the thermal stability of the PS/PEG membrane, causing of an increase of about 40-50 °C, where, the incorporation of Al_2O_3, CuO, SWCNTs and MWCNTs strengthened chemical bonds within the polymeric backbone. The TGA curves indicated that the thermal stability of the modified membranes was in order: PS/PEG/SWCNTs (M3) > PS/PEG/Al_2O_3 (M1) > PS/PEG/CuO (M2) > PS/PEG/MWCNTs (M4) > neat PS > PS/PEG. Therefore, PSF/PEG/SWCNTs membrane was the most stable membrane as compared with the other membranes.

3.1.5. Scanning electron microscope analysis

SEM images of the neat PS, PS/PEG, PS/PEG/Al_2O_3 (M1), PS/PEG/CuO (M2), PS/PEG/SWCNTs (M3) and PS/PEG/MWCNTs (M4) NC modified membranes are shown in Fig. 7. It can be realized that all membranes display an asymmetric assembly with a thick skin layer. Conversely, it is obvious that the kind of NPs considerably influenced the morphology of the NC membranes. It is found that the structure of neat PS membrane have a smooth and porous surface with a nano metric pore size and appear like rationally spongy in nature. The incorporation of different NPs causes coarser membrane surfaces, with certain aggregation of NPs Fig. 7. It is assumed that the incorporation of different type of NPs enhances the membranes surface possessions and creates new flow paths via the membrane surfaces, producing an improving in H_2O permeability and sorption. Most of the modified membranes looked more voids similar to tubes and condensed from spongy configuration.

The cross sections of the porous PS display a nodular, spongy and finger-like structure. A homogeneous propagation of the NPs in the polymer matrix is revealed on the surface, and there is tiny proof of NPs aggregations near the surface of the NC modified membranes.

3.2. Membrane distillation performance evaluation

3.2.1. Effect of membrane preparation conditions

3.2.1.1. Polymer concentration. The influence of PS flat sheet membrane preparation conditions such as PS monomer concentration, PS sheet thickness, operational temperatures, operational flow rate and feed water salinity was considered to observe the optimum preparation circumstances that provide best membrane performances. It is imperative to indicate that the most prepared membranes have salt retention more than 99.9%.

Polymer concentration in casting solution plays an imperative role in formative the membrane possessions (Hou, et al., 2014). To synthesize the polymer casting solution with various concentrations of PS pellets (w/v) were dissolved in DMF as a

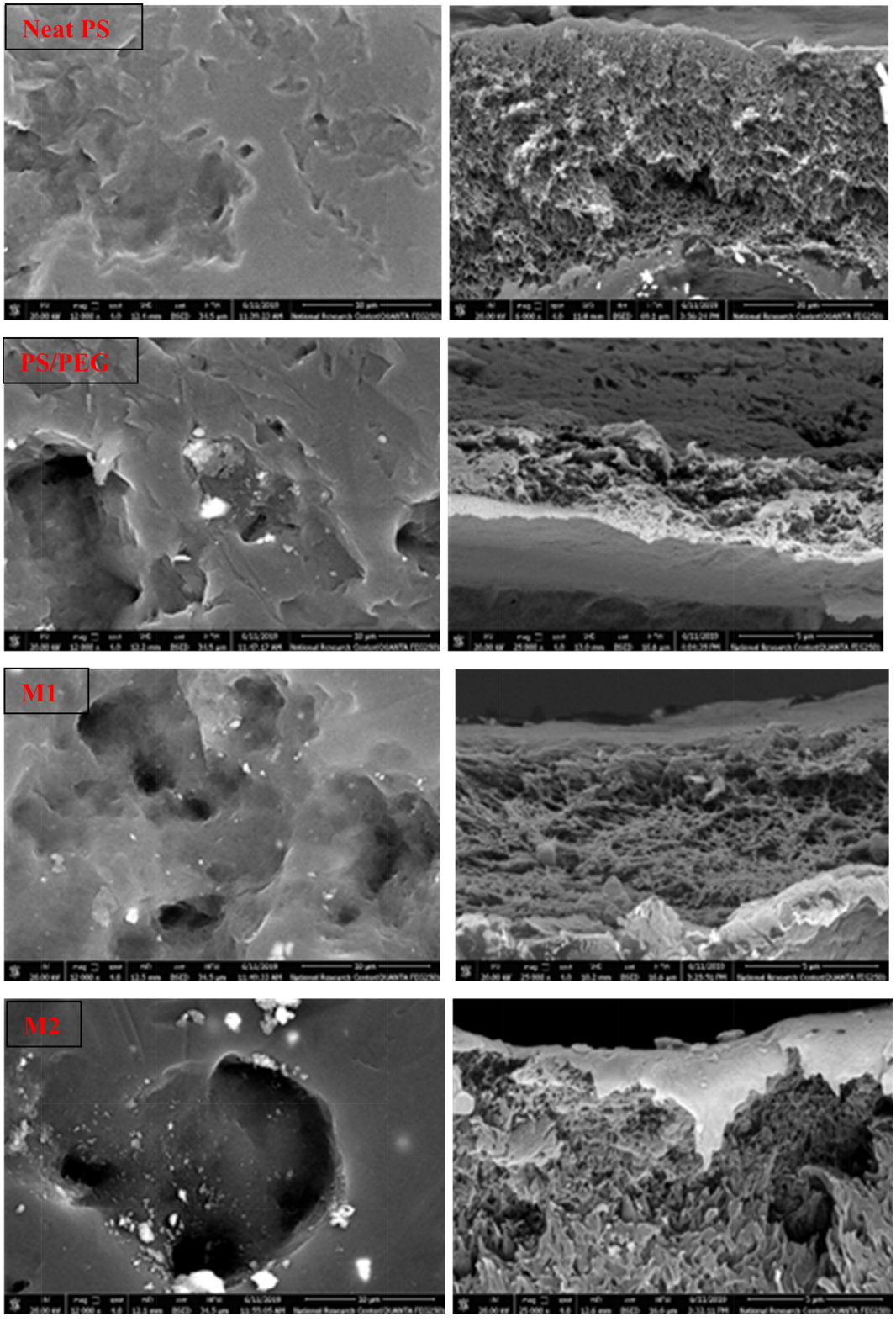

Fig. 7 SEM images of surface (left panel) and cross-sections (right panels) of the Neat PS, PS/PEG, PS/PEG/Al_2O_3 (M1), PS/PEG/CuO (M2), PS/PEG/SWCNTs (M3) and PS/PEG/MWCNTs (M4) NC modified membranes.

solvent. All synthetic PS flat sheet membranes were estimated using EDCMDS unit. Various PS monomer concentrations varied from 12 to 18 wt% were used to synthesized various MD membranes with same thickness of 100 μm. These membranes were performed using synthetic 20,000 mg/L NaCl as a feed solution. The experiments were achieved at flow rate 1 L/min and the temperature of both feed (T_f) and permeate (T_p) were 60 and 20 °C, respectively.

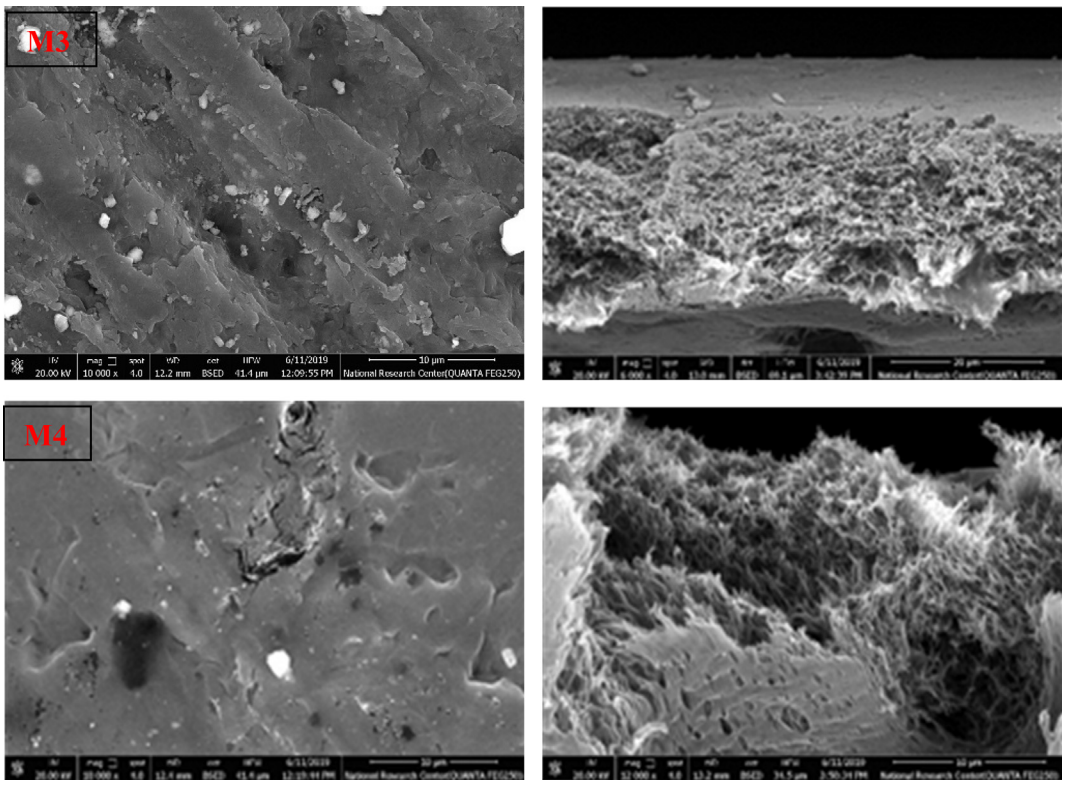

Fig. 7 (*continued*)

Fig. 8a displays enhanced PWF with increasing PS monomer concentrations from 12 to 16 wt%. Improved PWF may be attributable to the greater number of pores in membrane surfaces which lead to improve permeate flux (Zárate et al., 1995). Fig. 8a shows the PWF increased from 9 to 11.3 L/m^2.h as the polymer concentration increased from 12 to 16 wt%. This could be attributable to advance the membranes porosity and hydrophobicity as polymer concentration increases. Furthermore, this can be clarified that the higher values of PWF at 12 wt% PS monomer concentration could be owing to condensed water in the voids of the porous layer. Additional increasing the PS monomer concentration, beyond 16%, causes a decrease in PWF, where, intense polymerization procedures create a dense membrane with low porosity. Consequently, 16 wt% PS monomer concentration was selected as the optimum polymer concentration.

3.2.1.2. Effect of membrane thickness. The membrane thickness is an important representative in the EDCMDS, where there is an inversely relative relationship among the membrane thickness and the PWF (Khayet, 2011). Fig. 8b shows the influence of PS flat sheet membrane thickness on the EDCMDS PWF. Various PS membrane concentrations were synthesized with various thicknesses varied from 50 to 200 μm using an automated casting knife. All synthetic flat sheet membranes were casting at 50 μm were rejected due to the membranes become inconsistent and shows greater number of holes, which can be detected clearly against light and achieved higher PWF and the

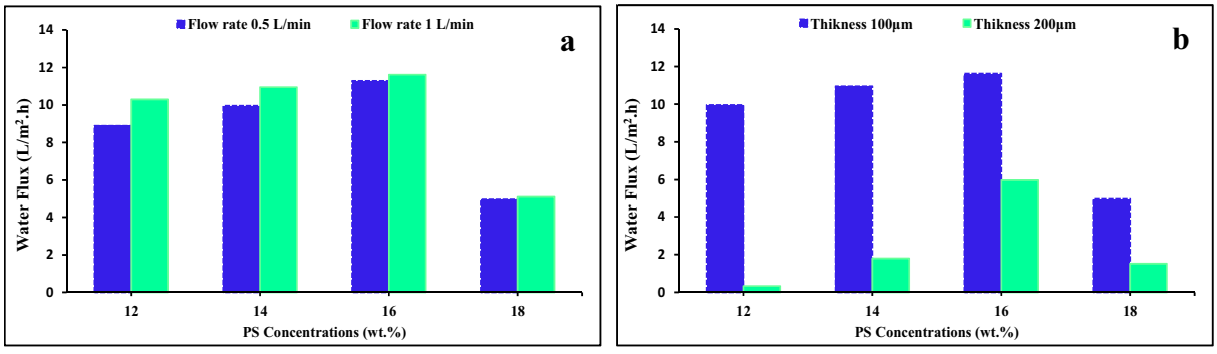

Fig. 8 Performance of membrane samples: (a) Effect of PS monomer concentration on the PWF with membrane thickness 100 μm; (b) Effect of PS membrane thickness on PWF using PS concentration = 16 wt%. These experiments were achieved using 20,000 mg/L NaCl as a feed solution at T_f = 60 °C, T_p = 20 °C, at flow rate = 1 L/min.

salt rejection was lower than 90%, which meant that these membranes were not suitable for EDCMDS procedure. The results display that the PS flat sheet membrane thicknesses inversely proportional with the number of pores into the membrane surfaces, i.e. the higher the number of pores in the membrane achieved due to lower PS polymer thickness which leads to decline the salt rejection and increase permeate flux (Zárate et al., 1995). The results show that PWF declined with increasing the membrane thickness from 100 to 200 µm using various PS concentrations from 12 to 18 wt%. These results approve that there is an inversely relationship among the membrane thickness, polymer concentration and the PWF, i.e. the PWF is decreased as the membrane becomes thicker, due to the mass transfer opposition of water molecules improved as well as heat loss during operation as a result of membrane thickness increases (Drioli et al., 2015). This can be mainly because of the greatest of membrane thickness mean growing on the polymer molecules that enhance the hydrophobicity properties which decline the membrane surface porosity. The membrane thickness of 50 µm was excluded because the membrane was very thin and easily cutted. Consequently, 16 wt% PS monomer concentration and thickness 100 µm was selected as the optimum polymer concentration and thickness.

3.2.2. *Effect of operating conditions for EDCMDS units*

There are different operations factors affecting the performances for the synthesized membranes among them feed and permeate temperatures, feed and permeate flow rates and feed water salinity.

3.2.2.1. Effect of feed temperature on PWF. Feed temperature (T_f) is an essential main influence in the operation procedure study where it doings as the driving force in membrane distillation technique. Fig. 9a displays the relation between the PWF and T_f for neat PS flat sheet membrane with 100 µm thickness at different polymer concentration varied from 12 to18 wt%. The experimentations were verified at flow rate was 1 L/min using 20,000 mg/L NaCl as feed water and permeate temperature 20 °C. The results shown that the feed water temperature increased from 40 to 60 °C and the PWF improved for all synthesized membrane with different polymer concentrations. Fig. 9a indicates that the PS flat sheet membrane with polymer concentration 16 wt% achieved higher PWF ranged from 7.1 to 11.63 L/m^2.h at T_f varied from 40 to 60 °C, respectively. This can be owing to the significant improved of the stream pressure of the feed solution with temperature, which improves the driving force therefore, the feed temperature has an important effect on the level of the PWF in membrane distillation procedure (Woo et al,. 2016). Furthermore, the membrane mass transfer factor and the membrane heat transfer factor enhance due to the temperature increased (Andrjesdóttir et al., 2013). This effect was attributed to the driving strength of mass transfer, which increase with increasing temperature of the feed vapor, So, 60 °C is the optimum feed temperature as in this temperature the membrane 16 wt% PS with thickness 100 µ gave higher permeate flux than the other polymer concentrations.

3.2.2.2. Effect of permeate temperature on PWF. Fig. 9b revealed that effect of the permeate temperature (T_p) on PWF. The T_p was ranged from 20 to 10 °C at different T_f ran-

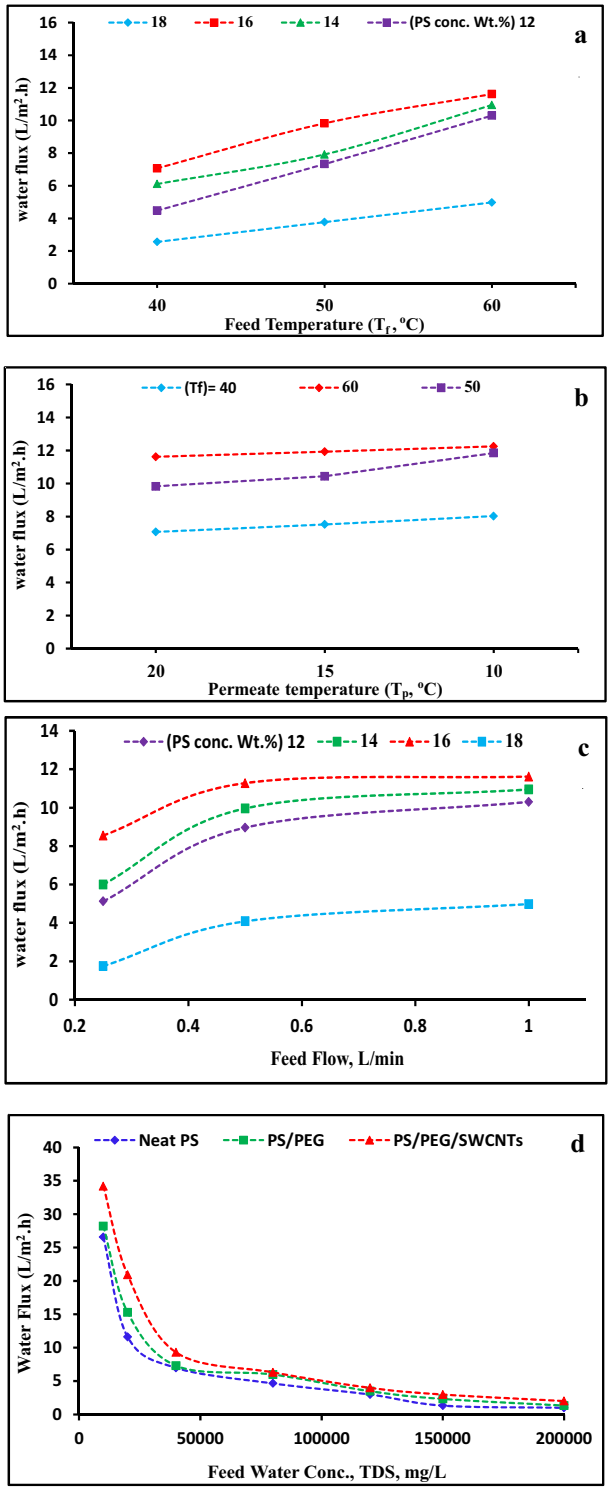

Fig. 9 Performance of membrane samples: (a) Effect of feed temperature (T_f) on the PWF at T_p = 20 °C; (b) Effect of permeate temperature (T_p) on the PWF at T_f ranged from 20 to 60 °C; (c) Effect of flow rate (L/min) on the PWF at T_f = 60 °C, T_p is 20 °C at different PS polymer concentrations (12, 14, 16 and 18 wt%); (d) Effect of feed salinity on PWF using Neat PS, PS/PEG and PS/PEG/SWCNTs membranes, PS concentrations = 16 wt%, T_f = 60 °C and T_p = 20 °C. All these experiments were achieved using 20,000 mg/L NaCl as a feed solution, at flow rate 1 L/min and membrane thickness 100 µm.

ged from 40 to 60 °C using 16 wt% PS at 100 μm thickness to display the influence of different T_p at different T_f. It was detected that as permeate temperature increases from 10 to 20 °C the water flux decrease at different T_f. These can be described as follow; as the vapor pressure variance in the EDCMDS procedure depend on the difference in the T_p and T_f, this is related to the decrease of the membrane vapor pressure (Shirazi et al., 2014). Conversely, if the feed stream temperature is kept constant, while varying the permeate stream temperature; it is more probable to have an improvement in membrane PWF attention to approach an asymptotic value at higher bulk phase temperature variances.

3.2.2.3. Effect of flow rate. During distillation process, the flow rate has a positive effect on the membrane water permeability; this is because of decreasing the temperature and concentration polarization effects onto the membrane surfaces. Furthermore, the excess in flow rate, i.e. feed circulation velocity or feed stirring rate increases the permeate flux (El-Bourawi et al., 2006; Manawi et al., 2014). The tests were verified at T_f = 60 °C and T_p = 20 °C with TDS 20,000 mg/L NaCl as a feed solutions. Fig. 9c explains the influence of flow rate (0.25, 0.5 and 1 L/min) on the PWF of the synthesized membranes at different PS polymer concentrations (12–18 wt%) of 100μ thickness. It was realized that the PWF of PS flat sheet membrane increased gradually as a function of flow rate increases for all polymer concentration. The outcomes show that increasing in the feed flow rate from 0.25 to 1 L/min improves the PWF from 8.6 to 11.63 L/m^2 h. These results mainly owing to improved volumetric flow rate which will improve the PWF. The liquid velocity increases when the volumetric flow rates rise, due to the convective heat transfer factor improves and the thermal surround layer thickness declines. Consequently, the temperature polarization influence decreases (Shirazi et al., 2012).

3.2.2.4. Effect of feed water salinity on flux. The feed water concentration is a more operational factor in any desalination procedure as value of feed salinity identifies what is the desalination procedure that could be practical in the desalination method. So the effect of feed concentration on PWF in EDCMDS technique depends mainly on the separation procedure itself. As it is well known EDCMDS can be utilized for the treatment of highly concentrated solutions without suffering the large drop in permeability observed in other membrane procedures such as the pressure energetic membrane procedures (Cath et al., 2004).

Fig. 9d shows the influence of feed water salinities which ranged from 10,000 to 200,000 mg/L on the PWF of the Neat PS, PS/PEG, and PS/PEG/SWCNTs flat sheet membranes. The results show that via increasing the feed salinity from 10,000 to 200,000 mg/L the PWF deceased from 26.6 to 1 L/m^2.h using neat PS, from 28.2 to 1.3 L/m^2.h using PS/PEG and from 34.2 to 2 L/m^2.h. The increase of the feed salinity results in a decline of the EDCMDS permeates flux. This behavior is mainly owing to the drop of the water vapor force and the driving force.

3.2.3. Effect of PEG and nanoparticles additive

The central goal of this research is to insert a new functional group via incorporation of different types of NPs, thereby enhancing the membrane surface structure and leads to improved membrane performance for produced water desalination.

Firstly, all the factors containing operating settings, and factors affecting on the neat PS membranes are adjusted. Formerly we enhancing the performances of PS membranes, exclusively in terms of improving permeate flux using various concentrations of PEG as pore forming agent, incorporation of various types of NPs such as; Al_2O_3, CuO, SWCNTs and MWCNT at adjusted circumstances. This carried out to examine the optimum circumstance that provides highest productivity contrary to feed temperature and feed salinity taking into concerns the salt retention of the synthesized membranes was superior to 99.9%.

The pure water flux (PWF) is examined to be the main specification feature for any membrane. PWF has a straight relationship with the quantity of pores and the top layer porosity of the membrane surface (Han and Nam, 2002). The effect of PEG on PWF at two flow rate (0.5 and 1) is shown in Fig. 10a and Table 3. It is obvious from Fig. 10a that PWF increases with increase in the dosage of PEG. The PWF of the neat Ps membrane is 11.3 and 11.6 L/m^2 h at flow rate 0.5 and 1 L/min, respectively, while with increasing the dosage of PEG from 0.5 to 2 wt% related to PS concentration (i.e. 16 wt%), the PWF is enhanced from 12 to 15.3 L/m^2.h at flow rate 1. The results demonstrate that the top layer porosity increases with increase in the dosage of PEG. The total number of pores increases and the pore size becomes more identical.

Further increasing the PEG monomer concentration, beyond 2%, leads to reduce in PWF and salt retention and produce a dense membrane with low porosity. This reduction in water flux may be owing to the creation of macro-voids in the polymer skin layer.

The highest goal of this investigation is to exist a novel functional group via embedding the four various NPs such as Al_2O_3, CuO, SWCNTs and MWCNTs. This incorporation indicates to enhance membrane performance for water desalination. These experiments were achieved via feed and permeate temperatures of 60 and 20 °C, respectively, where the flow rates of the feed and permeate ranged between 0.5 and 1 L/min respectively and feed salt concentration of 20,000 mg/L NaCl solution. The salt rejections (%) of acceptable outcomes were more than 99.9%.

Firstly, different PS/PEG/Al_2O_3 membranes were synthesized using different Al_2O_3 concentrations varied from 0.25 to 1 wt% as shown in Fig. 10b and Table 3. The DMF was selected to utilize as a best solvent for PS and PS/PEG, as well as an appropriate diffusion medium for the selected NPs. It is revealed that the improvement of PWF is conceivable via increasing Al_2O_3 concentration up to 0.75 wt% related to PS concentration (i.e. 16 wt%). It might be owing to the creation of void space resembling pipes which verifies the mass transmission procedure. Conversely, additional increasing of Al_2O_3; i.e. at 1 wt%, a decay in the PWF was detected. These mainly owing to the effect of hydrophilicity of Al_2O_3 NPs that began to show consequently pores blocking and pores wetting occur.

Secondly, the effect of CuO NPs concentration on PWF of PS/PEG membranes was considered using CuO concentrations varied from 0.25 to 1 wt% as revealed in Fig. 10c and Table 3.

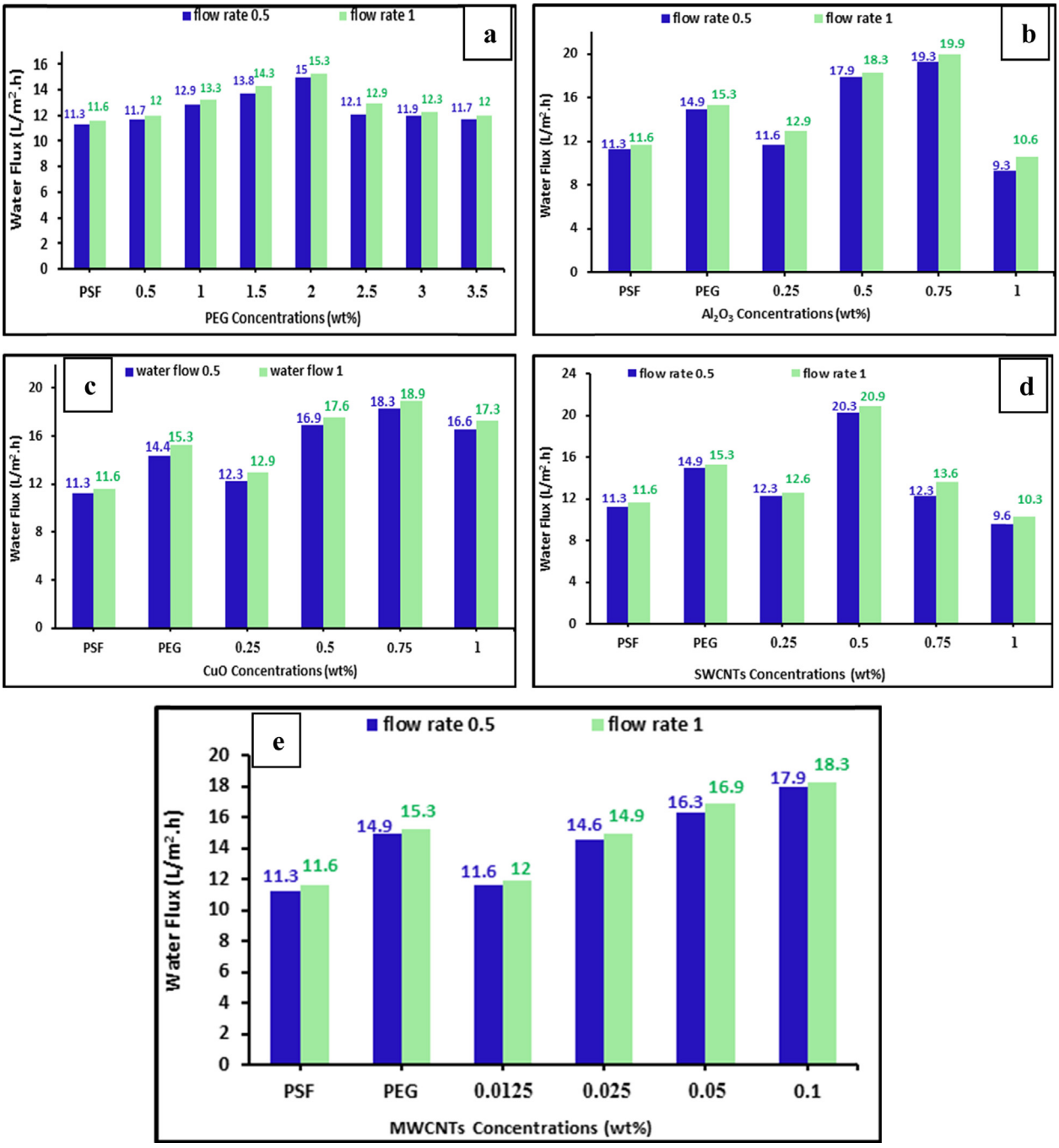

Fig. 10 (a) Effect of PEG concentration on PS membrane performance; (b) Effect of Al_2O_3 concentration on PSF/PEG membrane performance; (c) Effect of CuO NPs concentration on PS/PEG membrane performance; (d) Effect of SWCNTs concentration on PS/PEG membrane performance; (e) Effect of MWCNTs concentration on PS/PEG membrane performance. All these experiments where achieved at two different flow rate (0.5 and 1 L/min), using 20,000 mg/L NaCl as a feed solution at T_f = 60 °C, T_p = 20 °C and PS concentration 16 wt%, PEG concentration = 2 wt% and membrane thickness 100 μm.

It was clear that the PS/PEG/CuO NC modified membranes showed a significant increase in the PWF as compared with that of the neat PS and PS/PEG membranes where the best PWF was achieved using 0.75 wt% of CuO NPs concentrations. This might be owing to the creation of spongy and slight tear similar to pores in PS/PEG/CuO NC modified membrane. Conversely, a thicker and fewer permitted volume structure was achieved in membranes that synthesized using 0.25 and 1 wt% of CuO NPs.

Thirdly, different concentrations of SWCNTs as tubular nano-filler were incorporated onto PS/PEG polymer matrix where these concentrations ranged from 0.25 to 1 wt% related to PS concentration, (i.e. 16 wt%). The resulting PS/PEG/SWCNTs NC modified membranes were evaluated in term of water flux where the salt rejections (%) of acceptable outcomes were more than 99.9% as revealed in Fig. 10d and Table 3. It can be detected that the high permeate flux gained at 0.5 wt% of SWCNTs and start to decrease at 1 wt% when

Table 3 The permeate water flux (PWF) at two different flow rate L/min of the Neat PS, PS/PEG, PS/PEG/Al_2O_3 (M1), PS/PEG/CuO (M2), PS/PEG/SWCNTs (M3) and PS/PEG/MWCNTs (M4) NC modified membranes.

Membrane Types	Nanomaterials (wt%)	J_W (L/m^2 ·h) at flow rate 0.5 L/min	J_W (L/m^2 h) at flow rate 1 L/min
Neat PS	PS Conc. (16)	11.3	11.6
PS/PEG	PEG Conc. (2)	14.9	15.3
PS/PEG/Al_2O_3 (M1)	Al_2O_3 (0.75)	19.3	19.9
PS/PEG/CuO (M2)	CuO (0.75)	18.3	18.9
PS/PEG/SWCNTs (M3)	SWCNTs (0.5)	20.3	20.9
PS/PEG/MWCNTs (M4)	MWCNTs (0.1)	17.9	18.3

compared to the neat PS and PS/PEG membranes. However, the water flux decline using further SWCNTs concentrations (i.e. >0.5 wt%), this may be assign to combination of the NPs and a thicker film structure was created.

Finally, the performance of the membranes with various concentrations of MWCNTs as tubular nano-filler into PS/PEG using DMF as a solvent has been examined. Different concentrations of MWCNTs has been incorporated with PS/PEG mixtures which ranged from 0.0125 to 0.1 wt% regarding to PS concentrations, i.e. 16 wt%. All synthesized PS/PEG/MWCNTs NC modified membranes were estimated in DCMDS at two different flow rates as shown in Fig. 10e and Table 3. It can be obvious that all NC modified membranes displayed a substantial improve in the PWF when compared with the neat PS/PEG membrane. The enhancing in PWF was consistently linear with increasing MWCNTs concentrations. This improving in the PWF was attributable to increasing the porosity and the surface hydrophobicity of PS/PEG/MWCNTs NC modified membranes. This modification elevates membrane permeability and attracts water molecules that pass via the membrane matrix and improve PWF. Conversely, with additional increasing of MWCNTs concentrations i.e. greater than 0.1 wt% the performances of PS/PEG/MWCNTs NC modified membranes has been decayed this mainly attributed to a denser membrane structure is created which leads to increase the viscosity of the casting solution that produce a new membrane with a smaller pore size in addition to aggregation of MWCNTs and its contaminations (Moniruzzaman and Winey, 2006).

It can be concluded that the M3 membrane has the highest PWF compared with other three NC modified membranes using EDCMDS unit. The PWF is importantly affected by membrane morphology. Even though all the four synthesized membranes had finger-like cavities, macro-voids, the sponge-like structure of M3 membrane was extra porous, which significantly improved the membrane permeability and leads to improve the PWF. Furthermore, M3 NC modified membrane can reduce the resistance of mass transfer, consequently the higher permeate flux was achieved. Throughout the membranes permeability test procedures, the EC of the permeate starting from the neat PS, PS/PEG, M1, M2, M3 and M4 NC modified membranes were have the salt rejection achieved more than 99.99% this can be attributed to membrane surface possessions.

3.3. Stability of neat PS and PS/PEG/SWCNTs NC modified membranes

The performance stability is a very important factor for membrane distillation technique. For practical application, it is significant to maintain a stable performance for the prepared membrane for an extensive term operation. From the above-mentioned studies to the performance of various synthesized NC modified membranes, neat PS and M3 membranes were selected to be applied in 480 min continuous desalination process using EDCMDS to investigate their performance stability. Regeneration of the neat PS and M3 NC modified membranes without any changing in PWF is a very essential issue for the success of membrane distillation technology. To examine the performance stability of the M3 NC modified membrane compared to neat PS, a 480 min continuous desalination experiment of aqueous NaCl solution (20,000 mg/L) was directed with the T_f = 60 °C, T_p = 20 °C and the flow rates were fixed at 1 L/min other operating factors of the EDCMD procedure were in agreement with the permeability experiment. From the economic topic of outlook, it is estimated that such constituents could be used for several times without dropping their PWF, or at least with slight loss. The result of desalination performance is obtainable in Fig. 11. It can be seen that the permeate flux in M3 NC modified membrane maintain about 20 L/m^2 h throughout experiment and there are no observable changes of PWF. It can be showed that the PWF using neat PS and M3 NC modified membranes protect about 2 and 1.3 L/m^2 h, respectively throughout all the experiment procedure and there are a small observable decline of PWF about 18% and 6.5% using neat PS and M3 NC modified membrane, respectively.

Alternatively the neat PS displays that slow flux decline after 250 min the result specified that the membrane was partially wetted and salt rejection decline. The salt rejections (%) were initially fixed at 99.9% while at the end of the experimental shows a little decline using neat PS and M3 membranes

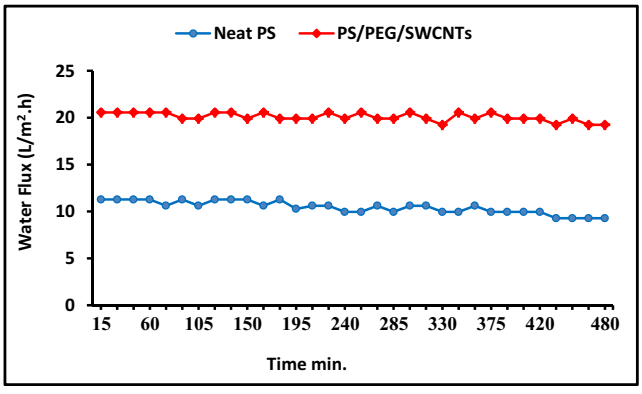

Fig. 11 The effect of operating time on PWF of neat PS and PS/PEG/SWCNTs NC modified membranes using 20,000 mg/L NaCl as a feed solution at T_f = 60 °C, T_p = 20 °C and PS concentration 16 wt%, PEG concentration = 2 wt% and membrane thickness 100 μm at flow rate 1 L/min.

where the S_R were about 99.90 and 99.95%, respectively. Conversely, the salt rejection has extremely reduced via operation time this means that there were some crystals created onto the membrane superficial (El-Bourawi et al, 2006).

This decline in PWF may be owing to the narrower pore size scattering of neat PS and M3 membranes. The experiment outcomes exposed that the M3 NC modified membrane had a stable permeability, salt rejection and it may be of magnificent prospective to be operated in the ECMDS procedure. It is concluded that the PWF of the M3 membrane showed higher stability (6.5% decline in PWF during all experiment) when compared to neat PS (18% decline). It is obvious that from the curve that M3 NC modified membrane exhibit long-term stability when compared to neat PS. The result showed that the synthesized M3 NC modified membrane could be successfully used for desalination using distillation technique when compared to neat PS membrane. The continuous desalination results displays that the NPs addition was not only beneficial for PWF improvement but also good for keeping performance stability of the modified membranes, and the M3 NC modified membrane may be of great potential to be utilized in the MD process.

4. Membrane application and produce water desalination

The oil field produce water include large quantities of heavy metals, inorganic salts, and naturally revolving radioactive substance are of specific environmental attention (Neff et al., 2011) consequently the desalination of oil field produce water can potentially conserve the environs and will deliver a fresh source of water. The invented membranes have been tested using the EDCMDS pilot scale laboratory unit to examine the membrane distillation performance and evaluate salt rejection. A Produce water sample, collected from Sarir oil field in Sirt basin, Libya, was used as a feed source in the EDCMDS unit using the synthesized sheet of PS/PEG/SWCNTs NC modified membrane. As of the aforementioned studies to the performance of different synthesized membranes, M3 membrane is selected for the desalination of oil field produce water sample. The M3 membrane thickness was 100 μm with PS and PEG polymer concentrations 16 wt% and 2 wt%, respectively and SWCNTs concentration 0.5 wt%. The feed Produce water and the distilled product water sample were analyzed for major ion ingredients to detect the efficiency of the membranes under the best operational conditions (T_f = 60 °C, T_p = 20 °C and the flow rates were fixed at 1 L/min. The initial produce water salinity and major ion concentrations are showed in Table 4 and Fig. 12.

The hydro-chemical species is reformed as to pH increased in the reject water sample than produce feed water sample after desalination Table 4 and Fig. 12. This increased related to change of HCO_3^- salt to CO_3^{2-} salt in water. Fig. 12 showed that the concentration of TDS, Ca^{2+}, Mg^{2+}, Na^+, K^+, SO_4^{2-} and Cl^- ions are increased owing to water extract via membrane distillation procedure. However the HCO_3^{2-} concentration was declined after desalination procedure this mainly attributed to change of bicarbonate salt to carbonate forms via increased the temperate as to equations:

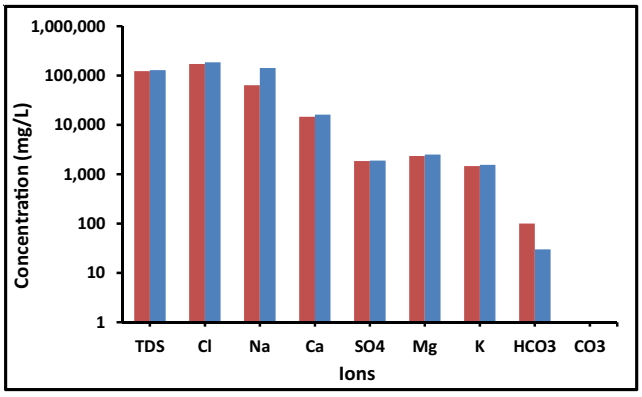

Fig. 12 Logarithmic diagram showing the membrane distillation performances for the PS/PEG/SWCNTs NC modified membranes. Produce water salinity (123,136 mg/L) has been used as feed water, at T_f = 60 °C, T_p = 20 °C and PS concentration 16 wt %, PEG concentration = 2 wt%, SWCNTs concentrations 0.5 wt % and membrane thickness 100 μm at flow rate 1 L/min.

$$2HCO_3^- \rightarrow CO_3^{2-} + CO_2 + H_2O \quad (4)$$

Conversely, the higher produce water salinity leads to make desalination via membrane distillation technique to disposal of these higher concentration salts. However after the desalination procedure, it is found that the synthesized M3 NC modified membrane was able to remove 99.99% of these salts with highly PWF. According to the significant improve of produce water desalination using M3 NC modified membrane, it can be therefore suggested that the M3 NC modified membrane could be used for desalination and treatment techniques.

5. Conclusions

In this work, the Polysulfone-Polyethylene glycol (PS/PEG) flat sheet membrane was synthesized via phase inversion technique using DMF as a solvent and distilled water was utilized as coagulant water bath. Polyethylene glycol (PEG) was utilized as the polymeric improver (2 wt%) and as a pore developing agent in the casting mixture. The PS membrane was cast from a homogeneous polymer solution having 16 wt% PS pellets and 84 wt% DMF and the resultant PS polymer

Table 4 Chemical analysis of major constituents of cations and anions of the water feed and reject MD desalination process using PS/PEG/SWCNTs NC modified membrane.

Parameter	pH	EC, mS/cm	TDS	Ca^{2+}	Mg^{2+}	Na^+	K^+	CO_3^{2-}	HCO_3^{2-}	SO_4^{2-}	Cl^-
			Mg/L								
Feed	5	192,400	123,136	14,700	2350	63,900	1470	0	100	1850	171,730
Rejected	6.6	202,700	129,728	16,270	2525	142,070	1555	35	30	1900	184,900

solution was casted with thickness 100 μm. Increased PS concentration and membrane thickness could decline membrane PWF. There is a confident impact at increase of the feed temperature and flow rate on the PWF. Conversely, there is a negative effect of the feed salt concentration and distillate temperature on the PWF of neat PS and PS/PEG membrane. The improvement of PS membrane was achieved through incorporation of PS/PEG with carbon-based nanomaterial e.g. MWCNTs, SWCNTs and inorganic nanoparticles, e.g. Al_2O_3 and CuO for EDCMD mediated water desalination. The incorporation of MWCNTs (0.1), SWCNTs (0.5), Al_2O_3 (0.75) and CuO (0.75 wt%) could significantly enhance the permeate flux of neat PS and PS/PEG membranes. The highest permeate flux achieved in the order of SWCNTs (20.91) > Al_2O_3 (19.92) > CuO (18.92) > MWCNT (18.20) > ($L/m^2{\cdot}h$) with optimized concentration of 0.5, 0.75, 0.75, 0.1 wt% relative to PS/PEG weight, i.e. 16%. The optimum effective circumstances involved feed and permeate temperatures 60 °C and 20 °C, respectively. The PS/PEG NC modified membranes revealed improved flux, salt rejection, mechanical properties and a stable permeability when compared with the neat PS and PS/PEG membranes. Among the nanocomposite membranes, PS/PEG/SWCNTs (0.5 wt%) showed highest flux of 20.91 ($l/m^2.h$). Thus, PS/PEG/SWCNTs NC membrane promises to be the best candidate in terms of quality and cost when compared to all prepared membranes for its potential application in water desalination. The PS/PEG/SWCNTs NC modified membrane with 0.5 wt% of SWCNTs used to treat produce water sample from Sarir oil field with flux 5.97 L/m^2 h. The experiment results revealed that the M3 NC modified membrane had a stable permeability, salt rejection and it may be of magnificent prospective to be operated in the MD procedure.

References

Abdelrasoul, A., Doan, H., Lohi, A., Cheng, C.H., 2015. Morphology control of polysulfone membranes in filtration processes: a critical review. Chem. Bio. Eng. Rev. 2 (1), 22–43.

Ahmadun, F.R., Pendashteh, A., Abdullaha, L.C., Biak, D.R.A., Madaeni, S.S., Abidin, Z.Z., 2009. Review of technologies for oil and gas produced water treatment. J. Hazard. Mater. 170, 530–551.

American Society for Testing Materials (ASTM), Water and environmental technology. Annual book of ASTM standards, U.S.A. Sec. 11, Vol.11.01and 11.02 West Conshohocken, (2002).

Andrjesdóttir, Ó., Ong, C.L., Nabavi, M., Paredes, S., Khalil, A.S.G., Michel, B., Poulikakos, D., 2013. An experimentally optimized model for heat and mass transfer in direct contact membrane distillation. Int. J. Heat Mass Transf. 66, 855–867.

Ang, W.L., Mohammad, A.W., Hilal, N., Leo, C., 2015. A review on the applicability of integrated/hybrid membrane processes in water treatment and desalination plants. Desalination 363, 2–18.

American Public Health Association (APHA), Standard methods for the examination of water and wastewater, 20th ed. Washington, DC, (1998) 46p.

Augustine, R., Malik, H.N., Singhal, D.K., Mukherjee, A., Malakar, D., Kalarikkal, N., Thomas, S., 2014. Electrospun poly caprolactone/ZnO nanocomposite membranes asbiomaterials with antibacterial and cell adhesion properties. J. Polym. Res. 21, 347. https://doi.org/10.1007/s10965-013-0347-6.

Balta, S., Sotto, A., Luis, P., Benea, L., Van der Bruggen, B., Kim, J., 2012. A new outlook onmembrane enhancement with nanoparticles: the alternative of ZnO. J. Membr. Sci. 389, 155–161.

Brown, E.M., Skougslad, W., Fishman, M.J., 1970. Methods for collection and analysis of water samples for dissolved minerals and gases Book 5, chap A1. U.S. Geological Survey Techniques for water resources investigations. USGS, Washington, DC.

Cath, T.Y., Adams, V.D., Childress, A.E., 2004. Experimental study of desalination using direct contact membrane distillation: a new approach to flux enhancement. J. Membr. Sci. 228 (2004), 5–16.

Celik, E., Park, H., Choi, H., Choi, H., 2011. Carbone nanotube blended polyethersulfone membranes for fouling control in water treatment. Water Res. 45, 274–282.

Daraei, P., Madaeni, S.S., Ghaemi, N., Salehi, E., Khadivi, M.A., Moradian, R., Astinchap, B., 2012. Novel polyethersulfone nanocomposite membrane prepared by PANI/Fe_3O_4 nanoparticles with enhanced performance for Cu(II) removal from water. J. Membr. Sci. 415–416, 250–259.

de Lannoy, C.-F., Soyer, E., Wiesner, M.R., 2013. Optimizing carnone nanoyub-reinforced polysulfone ultrafiltration membranes through carboxylic acid functionalization. J. Membr. Sci. 447, 395–402.

Domenico, P.A., Schwartz, F.W., 1990. Physical and chemicalhydrogeology. Wiley, New York, p. 824.

Dow, N., Zhang, J., Duke, M., Li, J., Gray, S.R., Ostarcevic, E., 2008. Membrane distillation of brine wastes. Research report no 63, CRC for water quality and treatment project no. 2.4.2.0 – Water treatment technologies. Water Qual. Res. Aust. Limited. ISBN 18766 1689X.

Drioli, E., Ali, A., Macedonio, F., 2015. Membrane distillation: recent developments and perspectives. Desalination 356, 56–84.

Du, R., Gao, B., Li, Y., 2013. Hydrophilic polysulfone film prepared from polyethylene glycol monomethylether via coupling graft. Appl. Surf. Sci. 274, 288–294. https://doi.org/10.1016/j.apsusc.2013.03.038.

El Bourawi, M.S., Ding, Z., Ma, R., Khayet, M., 2006. A framework for better understanding membrane distillation separation process. J. Membr. Sci. 285, 4–29.

El-Aassar, A.-H., Isawi, H., El-Noss, M., El-Kholy, R.A., Said, M.M., Shawky, H.A., 2019. Design and fabrication of continuous flow photoreactor using semiconductor oxides for degradation of organic pollutants. J. Water Process Eng. 32, 100922.

Elimelech, M., Phillip, W.A., 2011. The future of seawater desalination: energy, technology, and the environment. Science 333, 712–717.

Han, M.J., Nam, S.T., 2002. Thermodynamic and rheological variation in polysulfone solution by PVP and its effect in the preparation of phase inversion membrane. J. Membr. Sci. 202, 55–61.

Hem, J.D., 1991. Study and interpretation of the chemical characteristics of natural water. Scientific Publication, Jodhpur, India.

Homaeigohar, S., Elbahri, M., 2017. Graphene membranes for water desalination. NPG Asia Mater. 9, e427.

Hou, D., Fan, H., Jiang, Q., Wang, J., Zhang, X., 2014. Preparation and characterization of PVDF flat-sheet membranes for direct contact membrane distillation. J. Sep. Purificat. Technol. 135, 211–222.

Huang, Q., Liu, M., Zhao, J., Chen, J., Zeng, G., Huang, H., Tian, J., Wen, Y., Zhang, X., Wei, Y., 2017b. Facile preparation of polyethylenimine-tannins coated SiO2 hybrid materials for Cu2+ removal. Appl. Surf. Sci. https://doi.org/10.1016/j.apsusc.2017.08.233.

Huang, Q., Liu, M., Mao, L., Xu, D., Zeng, G., Huang, H., Jiang, R., Deng, F., Zhang, X., Wei, Y., 2017a. Surface functionalized SiO2 nanoparticles with cationic polymers via the combination of mussel inspired chemistry and surface initiated atom transfer radical polymerization: characterization and enhanced removal of organic dye. J. Colloid Interf. Sci. https://doi.org/10.1016/j.jcis.2017.03.102.

Huang, H., Liu, M., Xu, D., Mao, L., Huang, Q., Deng, F., Tian, J., Wen, Y., Zhang, X., Wei, Y., 2020. Facile fabrication of glycosylated and PEGylated carbon nanotubes through the combination

of mussel inspired chemistry and surface-initiated ATRP. Mater. Sci. Eng., C 106, 110157.
Isawi, H., 2018. Development of thin-film composite membranes via radical grafting with methacrylic acid/ ZnO doped TiO_2 nanocomposites. React. Funct. Polym. 131, 400–413.
Isawi, H., 2019. Evaluating the performance of different nano-enhanced ultrafiltration membranes for the removal of organic pollutants from wastewater. J. Water Process Eng. 31, 100833.
Isawi, H., El-Sayed, M.H., Feng, X., Shawky, H., Abdel, M.S., 2016b. Mottaleb, Surface nanostructuring of thin film composite membranes viagrafting polymerization and incorporation of ZnO nanoparticles. Appl. Surf. Sci. 385, 268–281.
Isawi, H., El-Sayed, M.H., Eissa, M., Shouakar-Stash, O., Shawky, H., Mottaleb, M.S.A., 2016a. Integrated geochemistry, isotopes, and geostatistical techniques to investigate groundwater sources and salinization origin in the Sharm EL-Shiekh Area, South Sinia. Egypt. Water Air Soil Pollut. 227 (5), 151. https://doi.org/10.1007/s11270-016-2848-5.
Jung, B., Yoon, J.K., Kim, B., Rhee, H.W., 2004. Effect of molecular weight of polymeric additives on formation, permeation properties and hypochlorite treatment of asymmetric polyacrylonitrile membranes. J. Membr. Sci. 243, 45–57.
Khalkhali, R.A., Keivani, M.B., 2005. Thermogravimetry analysis of electrochemically synthesized polypyrrole conducting polymer films. Asian J. Chem. 17, 1483.
Khayet, M., 2011. Membranes and theoretical modeling of membrane distillation: a review. Adv. Colloid Interface Sci. 164, 56–88.
Lai, G.S., Lau, W.J., Goh, P.S., Ismail, A.F., Yusof, N., Tan, Y.H., 2016. Graphene oxide incorporated thin film nanocomposite nanofiltration membrane for enhanced salt removal performance. Desalination 387, 14–24.
Lau, W.J., Ismail, A.F., Misdan, N., Kassim, M.A., 2012. A recent progress in thin film composite membrane: a review. Desalination 287, 190–199.
Leo, C.P., Lee, W.P.C., Ahmed, A.L., Mohammad, A.W., 2012. Polysulfone membranesblended with ZnO nanoparticals for reducing fouling by oleic acid. Sep. Purif. Technol. 89, 51–56.
Liu, F., Hashim, N.A., Liu, Y., Abed, M.M., Li, K., 2011. Progress in the production and modification of PVDF membranes. J. Membr. Sci. 375 (1), 1–27.
Ma, Y., Shi, F., Ma, J., Wu, M., Zhang, J., Gao, C., 2011. Effect of PEG additive on the morphology and performance of polysulfone ultrafiltration membranes. Desalination 272, 51–58.
Madaeni, S., Zinadini, S., Vatanpour, V., 2013. Preparation of super hydrophobic nanofiltration membrane by embedding multi walled carbon nanotube and poly dimethyl siloxane in pores of microfiltration membrane. Sep. Purif. Technol. 111, 98–107.
Manawi, Y.M., Khraisheh, M.A.M.M., Fard, A.K., Benyahia, F., Adham, S., 2014. A predictive model for the assessment of the temperature polarization effect in direct contact membrane distillation desalination of high salinity feed. Desalination 341, 38–49.
Mo, J., Son, S.H., Jegal, J., Kim, J., Lee, Y.H., 2007. Preparation and characterization ofpolyamide nanofiltration composite membranes with TiO_2 layers chemically connectedto the membrane surface. J. Appl. Polym. Sci. 105, 1267–1274.
Moniruzzaman, M., Winey, K.I., 2006. Polymer nanocomposites containing carbon nanotubes. Macromolecules 39, 5194–5205.
Moniruzzaman, M., Chattopadhyay, J., Billups, W.E., Winey, K.I., 2007. Tuning themechanical properties of SWNT/nylon 6 10 composites with flexible spacersat the interface. Nano Lett. 7 (5), 1178–1185.
Mosqueda-Jimenez, D.B., Narbaitz, R.M., Matsuura, T., Chowdhury, G., Pleizier, G., Santerre, J.P., 2004. Influence of processing conditions on the properties of ultrafiltration membranes. J. Membr. Sci. 231, 209–224.
Nechifor, A., Panait, V., Naftanaila, L., Batalu, D., Voicu, S., 2013. Symmetrically polysulfone membranes obtained by solvent evaporation using carbon nanotubes as additives.Synthesis, characterization and applications. Dig. J. Nanomater. Biostruct. 8, 875–884.
Neff, J., Lee, K., De Blois, E.M., 2011. Produced Water: Overview of Composition, Fates, and Effects. Springer, New York, NY.
Okiel, K., El-Aassar, A.H.M., Temraz, T., El-Etriby, S., Shawky, H. A., 2016. Performance assessment of synthesized CNT/polypropylene composite membrane distillation for oil field produced water desalination. Desalin. Water Treat. 57, 10995–11007.
Pana, C.-Y., Xua, G.-R., Xua, K., Zhaoa, H.-L., Wua, Y.-Q., Sua, H.-C., Xua, J.-M., Das, R., 2019. Electrospunnano fibrous membranes in membrane distillation: recent developments and future perspectives. Sep. Purif. Technol. 221, 44–63.
Sadtler, the Infrared Spectra Atlas of Monomers and P-3-N. Kwon andpolymers: Sadtler Research Laboratories (1980).
Salehi, E., Madaeni, S.S., Rajabi, L., Vatanpour, V., Derakhshan, A. A., Zinadini, S., Ghorabi, S., Monfared, H.A., 2012. Novel chitosan/poly(vinyl)alcohol thin adsorptive membranes modified with amino functionalized multi-walled carbone nanitubes from Cu(II) removal from water: preparation, characterization, adsorption kinetics and thermodynamics. Sep. Purif. Technol. 89, 309–319.
Saljoughi, E., Amirilargani, M., Mohammadi, T., 2010. Effect of PEG additive and coagulation bath temperature on the morphology, permeability and thermal/ chemical stability of asymmetric CA membranes. Desalination 262, 72–78.
Shirazi, M.M.A., Kargari, A., Shirazi, M.J.A., 2012. Direct contact membrane distillation for seawater desalination. Desalin. Water Treat. 49 (1–3), 368–375.
Shirazi, M.M.A., Kargari, A., Tabatabaei, M., 2014. Evaluation of commercial PTFE membranes in desalination by direct contact membrane distillation. Chem. Eng. Process. 76, 16–25.
Singh, P.S., Joshi, S.V., Trivedi, J.J., Devmurari, C.V., Rao, A.P., Ghosh, P.K., 2006. Probing the structural variations of thin film composite RO membranes obtained by coating polyamide over polysulfone membranes of different pore dimensions. J. Membr. Sci. 278, 19–25.
Subramani, T., Elango, L., Damodarasamy, S.R., 2005. Groundwater quality and its suitability for drinking and agricultural use in Chithar River Basin, Tamil Nadu India. Environ. Geol. 47, 1099–1110.
Susanto, H., Ulbricht, M., 2009. Characteristics, performance and stability of polyethersulfoneultrafilteration membranes prepared by phase separation method using different macromolecular additives. J. Membr. Sci. 327, 125–135.
Tang, E., Cheng, G., Ma, X., 2006. Preparation of nano-ZnO/PMMA composite particles via grafting of the copolymer onto the surface of zinc oxide nanoparticles. Powder Technol. 161, 209–214.
Vetrivel, V., Rajendran, K., Kalaiselvi, V., 2015. Synthesis and characterization of pure titanium dioxide nanoparticles by sol-gel method. Int. J. ChemTech Res. 7, 1090–1097.
Woo, Y.C., Kim, Y., Shim, W., Tijing, L.D., Yao, M., Nghiem, L.D., Choi, J., Kim, S., Shon, H.K., 2016. Graphene/PVDF flat-sheet membrane for the treatment of RO brine from coal seam gas produced water by air gap membrane distillation. J. Membr. Sci. 513, 74–84.
Wu, H., Shen, F., Wang, J., Wan, Y., 2018. Membrane fouling in vacuum membrane distillation for ionic liquid. J. Membr. Sci. 550, 436–447.
Xu, Z.-L., Chung, T.-S., Loh, K.-C., Lee, B.C., 1999. Polymeric asymmetric membranes made from polyetherimide/polybenzimidazole/poly(ethyleneglycol) (PEI/PBI/PEG) for oil–surfactant–water separation. J. Membr. Sci. 158, 41–53.
Yuenyao, Chalad, Chittrakarn, Thawat, Tirawanichakul, Yutthana, Sirijarukul, Suksawat, 2016. surface modification of asymmetric polysulfone/polyethylene glycol membranes by DC Ar-glow discharge plasma. Int. J. Polymer Sci. 2016, 1–8. https://doi.org/10.1155/2016/4759150.

De Zarate, J.O., Pen, L., Mengual, J.I., 1995. Characterization of membrane distillation membranes prepared by phase inversion. Desalination 100 (1–3), 139–148.

Zeng, G., Liu, X., Liu, M., Huang, Q., Xu, D., Wan, Q., Huang, H., Deng, F., Zhang, X., Wei, Y., 2016. Facile preparation of carbon nanotubes based carboxymethyl chitosan nanocomposites through combination of mussel inspired chemistry and Michael addition reaction: characterization and improved Cu^{2+} removal capability. J. Taiwan Inst. Chem. Eng. 68, 446–454.

Zeng, G., Chen, T., Huang, L., Liu, M., Jiang, R., Wan, Q., Dai, Y., Wen, Y., Zhang, X., Wei, Y., 2018a. Surface modification and drug delivery applications of MoS2 nanosheets with polymers through the combination of mussel inspired chemistry and SET-LRP. J. Taiwan Inst. Chem. Eng. 82, 205–213.

Zeng, G., Huang, L., Huang, Q., Liu, M., Xu, D., Huang, H., Yang, Z., Deng, F., Zhang, X., Wei, Y., 2018b. Rapid synthesis of MoS2-PDA-Ag nanocomposites as heterogeneous catalysts and antimicrobial agents via microwave irradiation. Appl. Surf. Sci. https://doi.org/10.1016/j.apsusc.2018.07.144.

Zhang, X., Huang, Q., Liu, M., Tian, J., Zeng, G., Li, Z., Wang, K., Zhang, Q., Wan, Q., Deng, F., Wei, Y., 2015. Preparation of amine functionalized carbon nanotubes via abioinspired strategy and their application in Cu^{2+} removal. Appl. Surf. Sci. 343, 19–27.

Zhang, X., Huang, Q., Deng, F., Huang, H., Wan, Q., Liu, M., Wei, Y., 2017. Mussel-inspired fabrication of functional materials and their environmentalapplications: progress and prospects. Appl. Mater. Today 7, 222–238.

Zheng, J., Ozisik, R., Siegel, R.W., 2005. Disruption of self-assembly and altered mechanical behavior in polyurethane/zinc oxide nanocomposites. Polymer 46, 10873–10882.